Wagner Francisco Rezende Cano

Aplicação da Análise de Séries Temporais para Detecção e Prognóstico de Danos em Estruturas Inteligentes

Ilha Solteira

2015

UNIVERSIDADE ESTADUAL PAULISTA "JULIO DE MESQUITA FILHO"
FACULDADE DE ENGENHARIA
CAMPUS DE ILHA SOLTEIRA

Wagner Francisco Rezende Cano

Aplicação da Análise de Séries Temporais para Detecção e Prognóstico de Danos em Estruturas Inteligentes

Dissertação apresentada ao Programa de Pós-Graduação em Engenharia Mecânica, Faculdade de Engenharia Mecânica de Ilha Solteira – UNESP como parte dos requisitos necessários para obtenção do título de Mestre em Engenharia Mecânica.
Área do Conhecimento: Mecânica dos Sólidos.

Orientador: Prof. Dr. Samuel da Silva

Ilha Solteira

2015

FICHA CATALOGRÁFICA
Desenvolvido pelo Serviço Técnico de Biblioteca e Documentação

Cano, Wagner Francisco Rezende.
C227a Aplicação da análise de séries temporais para detecção e prognóstico de danos em estruturas inteligentes / Wagner Franciso Rezende Cano. – Ilha Solteira: [s.n.], 2015
67 f. : il.

Dissertação (mestrado) – Universidade Estadual Paulista. Faculdade de Engenharia de Ilha Solteira. Área de conhecimento: Mecânica dos Sólidos, 2015

Orientador: Samuel da Silva
Inclui bibliografia

1. Monitoramento estrutural. 2. Propagação de ondas. 3. Séries temporais. 4. Estruturas inteligentes.

unesp UNIVERSIDADE ESTADUAL PAULISTA
CAMPUS DE ILHA SOLTEIRA
FACULDADE DE ENGENHARIA DE ILHA SOLTEIRA

CERTIFICADO DE APROVAÇÃO

TÍTULO: Application of Time Series Analysis for Damage Detection and Prognosis in Smart Structures

AUTOR: WAGNER FRANCISCO REZENDE CANO
ORIENTADOR: Prof. Dr. SAMUEL DA SILVA

Aprovado como parte das exigências para obtenção do Título de Mestre em Engenharia Mecânica , Área: MECANICA DOS SOLIDOS, pela Comissão Examinadora:

Prof. Dr. SAMUEL DA SILVA
Departamento de Engenharia Mecânica / Faculdade de Engenharia de Ilha Solteira

Prof. Dr. MICHAEL JOHN BRENNAN
Departamento de Engenharia Mecânica / Faculdade de Engenharia de Ilha Solteira

Prof. Dr. ROBERTO GIL ANNES DA SILVA
Comando-Geral de Tecnologia Aeroespacial / Instituto Tecnológico de Aeronáutica

Data da realização: 12 de maio de 2015.

Acknowledgments

First of all, I wold like to thank my parents, Solange and Wagner, and family for all the support throughout such special moment of my life. Also, I am thankful for the company and help of my girlfriend Camila.

I am thankful to Professor Samuel da Silva for the opportunity to keep developing my research. I am also thankful to Professor Vicente Lopes Júnior, Professor João Antonio Pereira and Professor Mike Brennan for the advises which were very useful to accomplish this work.

I would like to thank the members of GMSINT and Carlos “Grilo” Santana for always being helpful and to contribute to my academic and personal growth.

I am thankful to the SHM staff of CPqD – Paulo Henrique de Oliveira Lopes, Bernardo José Guilherme de Aragão and Edmilson Sanches Silva – for offering their lab and expertise. I am also pleased for the opportunity to be part of their staff.

I would like to acknowledge the financial support provided by the following Brazilian funding agencies: Research Foundation of São Paulo (FAPESP) by grant number 12/09135-3 and National Council for Scientific and Technological Development (CNPq) by grant number 470582/2012-0.

I am also thankful to FAPEMIG and CNPq for partially funding the present research work through the National Institute of Science and Technology in Smart Structures in Engineering (INCT-EIE).

Finally, I am thankful to the Coordination for Higher Education Staff Development (CAPES) for my scholarship. The supplying of the “SMART layers” from Acellent Technologies® is also very much appreciated.

Resumo

Esse trabalho apresenta uma abordagem baseada no processamento de séries temporais para tratar o problema de detecção e o prognóstico de danos em estruturas com sensores e atuadores piezelétricos acoplados considerando as possíveis variabilidades ambientais e operacionais. A primeira abordagem se baseia na identificação de um modelo autorregressivo de predição construído com um sinal temporal de resposta de referência. Métricas indicativas de danos são extraídas dos erros de predição e a separação de efeitos (carregamento ou danos) é feita por um algoritmo de agrupamento fuzzy. Esse procedimento é implementado em uma estrutura de material compósito ensaiada em um sistema para teste de materiais de modo a reproduzir condições de carregamento a fim de simular condições reais de operação da estrutura. Por outro lado, a segunda metodologia proposta emprega uma identificação de dois estágios. Primeiramente, um modelo autorregressivo é criado para o monitoramento estrutural como no procedimento anterior, porém, utilizando o controle estatístico de processos para detectar um dano progressivo. Em seguida, modelos autorregressivos com entradas exógenas são estimados para as condições de referência e de dano para acompanhar as variações de parâmetros e permitir a realização de um prognóstico sobre a condição estrutural futura da estrutura. Testes iniciais em uma placa de alumínio mostraram que este método é capaz de realizar um prognóstico razoável e predizer o comportamento dinâmico da estrutura associado com um nível específico de redução de massa. Ambos métodos e resultados são discutidos e comparados ao final do trabalho.

Palavras-chave: Monitoramento de integridade estrutural. Variabilidades. Séries temporais. Ondas de Lamb. Prognóstico.

Abstract

This work presents an approach based on time series processing to deal with the damage detection and prognosis issue in structures coupled with piezoelectric sensors and actuators considering eventual operational and environmental variabilities. The first approach is based on the identification of a predictive autoregressive model obtained with a reference time response. Damage indicative metrics are extracted from prediction errors and the separation of effects (loading or damage) is performed by a fuzzy clustering algorithm. This procedure is carried on a composite structure attached to a material test system to reproduce loading conditions in order to simulate real operational conditions. On the other hand, the second proposed methodology employs a two step identification. First, an autoregressive model is created for structural monitoring similarly to the previous procedure, but employing statistical process control to detect progressive damage. Next, autoregressive models with exogenous inputs are estimated for reference and damaged conditions in order to track variation of parameters, allowing the prognosis of the structure's future structural condition. Initial tests on an aluminum plate indicated that this method is capable of performing a reasonable prognosis and predicting structure's dynamic behavior associated to a specific level of mass reduction. Both methods and results are discussed and compared by the end of the work.

Keywords: Structural health monitoring. Variabilities. Time series. Lamb waves. Prognosis.

List of Symbols

$\mathbf{A}$ – Norm-inducing matrix
A – Polynomial acting on the output signal
a – Coefficient of polynomial A
B – Polynomial acting on the input signal
C – Centroid of a cluster
c – Number of clusters
c_L – Lamb wave longitudinal mode velocity
c_P – Lamb wave phase velocity
c_T – Lamb wave transverse mode velocity
e – Discrete prediction error vector (V)
f – Discrete frequency vector (Hz)
h – Plate thickness
J – Function to be minimized by the fuzzy clustering analysis
$\mathbf{j}$ – imaginary number
k – Discrete sample
l – Discrete sample
m – Number of elements in a damage index subgroup
N – Number of samples or realizations
n – Number of damage index subgroups
n_a – Number of a coefficients
n_b – Number of b coefficients
n_θ – Number of estimated coefficients
p – Relative position of clusters
q – Backshift operator
S – Mean of S_i values
S_i – Standard deviation of each damage index subgroup
t – Discrete time vector (s)
$\mathbf{U}$ – Left singular vector
u – Discrete input signal vector (V)
$\mathbf{V}$ – Right singular vector

$\overline{X}_i$	–	Mean of each damage index subgroup
x	–	Feature index
y	–	Discrete output signal vector (V)
$\hat{y}$	–	Vector y adjusted by an autoregressive model (V)
$Z_{\alpha/2}$	–	Number of standard deviations for the X-bar control chart

Greek Letters

γ	–	γ index
$\bar{\gamma}$	–	Mean γ index
ξ	–	Wavenumber
μ	–	Mean operator
σ	–	Standard deviation operator
$\mathbf{\Sigma}$	–	Diagonal matrix from the single value decomposition
$\mathbf{\Sigma}_{ii}$	–	Diagonal terms of matrix $\mathbf{\Sigma}$
ω	–	wave circular frequency

List of Abbreviations

ACF	–	Autocorrelation function
AIC	–	Akaike's information criterion
AR	–	Autoregressive model
$ARMA$	–	Autoregressive moving average model
ARX	–	Autoregressive model with exogenous inputs
BSS	–	Baseline signal stretch
$CCDM$	–	Correlation coefficient deviation metric
CL	–	Center line
$CPqD$	–	*Centro de Pesquisa e Desenvolvimento em Telecomunicações*
FPE	–	Final prediction error
MTS	–	Material test system
OBS	–	Optimum baseline selection
PZT	–	Piezoelectric transducer
SEM	–	Spectral element model
SHM	–	Structural Health Monitoring
$STFT$	–	Short time Fourier transform
UCL	–	Upper control limit

List of Figures

List of Tables

Contents

1 Introduction

The process of applying damage detection methods for aerospace, civil and mechanical structures is commonly called Structural Health Monitoring – SHM (FARRAR; WORDEN, 2007; WORDEN et al., 2007; FIGUEIREDO et al., 2009). Economic benefits are the main driving force for the implementation of such strategies due to their capacity to reduce operational cost (CHANG et al., 2003; FARRAR; LIEVEN, 2007). Additionally, life safety is a crucial issue since many aging technical infrastructure are still operant despite of the risk of failure which is increased by damage accumulation (FARRAR; WORDEN, 2007; FASSOIS; SAKELLARIOU, 2007).

Traditional non destructive testing is often time consuming and carried by specialized workers. Moreover, these procedures are also performed in inaccessible spots requiring disassemble what could itself result in the introduction of damage to the structure. Besides, an online monitoring system would identify damage before it became hazard to the normal operation of the structure.

It is known that all materials have inherent defects caused by imperfections and manufacturing flaws that due to aging and degradations processes can generate damage (WORDEN et al., 2007). As stated by Worden and Dulieu-Barton (2004), damage causes a non ideal operation of the structure whose propagation could lead to fault. The rate of damage growth depends on the operational and environmental conditions that the structure is subjected. Thus, because of its gradual evolution, a specific level of damage has to be defined beyond what the structure will no longer operate in an acceptable manner. This integrity analysis relies on the extraction of damage-sensitive features from measured signals. However, the variety of operational and environmental conditions that real world structures are subjected also causes measurement variability which often affects signal features as well (SOHN, 2007; FRITZEN; KRAEMER, 2009).

Therefore, a robust in-service monitoring technique must be able to distinguish between changes causes by damage and those caused by other conditions avoiding false-positive indication diagnosis (CROSS et al., 2011). A common strategy is to collect datasets over a wide range of operational and environmental conditions experienced by the monitored structure (SOHN, 2007; FIGUEIREDO et al., 2011). Therewith, the development of mechanisms to extract exclusively damage-sensitive features still is a technical challenge (FARRAR; WORDEN, 2007; FIGUEIREDO et al., 2011).

The previous fact evidences the absence of SHM methods and standards for real world structures besides those that deal with the condition monitoring of rotating machinery in which the application relies on pattern recognition of the measurements, often in a qualitative fashion, without the need of models for damage identification. Also, for this kind of devices damage type and location are normally known, facilitating signal acquisition and processing which enables the prediction of the device's future behavior (FARRAR; WORDEN, 2007).

This estimation of the remaining useful life of a structure is referred as damage prognosis which can be interpreted as the progress of SHM techniques that simply provide the identification of damage. The procedure is based on the quantification of the damage present in a structure through the development of predictive models to track structural integrity (FARRAR, 2003; FARRAR; LIEVEN, 2007). The prognosis is achieved by integrating information about operational and environmental conditions and damage presence/evolution in order to optimize service life (FARRAR, 2003).

In this context, one of the greatest current challenges to the application of SHM techniques is the development of algorithms capable of both detect damage in the presence of measurement variability and enable prognosis without the need of intricate physics or mathematical based models, for example by using finite element methods or boundary element methods. In this sense, the present work aims to contribute with the employment of autoregressive models associated to response signals with Lamb wave excitation. This modeling is a simple regressive emulator based on time series to describe the behavior and to detect possible structural changes.

1.1 Objectives

The goal of this work is to describe and to test an approach based on time series analysis for damage detection and prognosis in smart structures considering possible operational and environmental variabilities. The first method used a reference autoregressive model and fuzzy clustering whereas the second one employed a two step identification for the extrapolation of autoregressive models.

1.2 Outline of the Work

The present work is organized in the following sections:

- Chapter 1: **Introduction** provides the motivation for SHM and an overview about the challenges for the implementation of damage detection and prognosis strategies for real world structures;
- Chapter 2: **Operational and Environmental Variability and Damage Prognosis** presents an investigation of relevant works that deal with crucial issues related to reliable structural monitoring;
- Chapter 3: **Damage Detection in Composite Materials Considering Loading Effect** describes a robust damage detection technique based on clustering analysis in order to separate distinct effects on the structure's response;
- Chapter 4: **Damage Prognosis using Autoregressive Models** presents the development of a damage detection procedure based on statistical process control and a coefficient extrapolation method capable of reproducing structural behavior of a specific damage level present in an aluminum plate;
- Chapter 5: **Final Remarks** provides the main conclusions of this work and suggestion for future research.

Also, supplementary theoretical topics are provided in the following appendixes:

- APPENDIX A – Lamb Waves;
- APPENDIX B – Autoregressive Models;
- APPENDIX C – Time-Frequency Analysis – Trace Index;
- APPENDIX D – Fuzzy Clustering Analysis.

2 Operational and Environmental Variability and Damage Prognosis

In this chapter the basic aspects for the development of SHM techniques and the paradigm of vibration-based methods for damage detection are presented. Also, the influence of operational and environmental conditions in measurement variability is explained. Finally, the concept of damage prognosis for the optimization of useful life is described.

2.1 Overview of the SHM Process

One of the challenges to become SHM an actual practice is to develop mechanisms to discriminate changes caused by damage from those caused by operational and environmental conditions (FARRAR; WORDEN, 2007). To meet such requirement, first it is needed to present the basic aspects of SHM techniques. Rytter and Kirkegaard (1994) defined four categories related to the stage of a SHM process in a structure:

1. Detection of damage;
2. Localization of damage;
3. Identification of the damage type;
4. Quantification of the damage severity.

According to Inman (2001), the incorporation of intelligent materials in a structure leads to three more levels:

5. Combines level 4 with smart structures for self-diagnosis;
6. Combines level 4 with smart structures and control to create an auto-repair system;

7. Combines level 1 with active control and smart structures for a control and monitoring simultaneous system.

Obviously, it is desirable to reach the top level of monitoring in an attempt to improve system reliability. However, it is important to note that even the first stage of monitoring is not trivial for many real-world applications due to many changing factors around the structure. Also, economic factors play an important role since the amount of transducers and hardware investment may cause the application of the monitoring prohibitive. A feasible way to overcome this adversity is through the application of vibration-based methods which are explained in the following section.

2.2 Vibration-Based Methods for Damage Detection

After the definition of stage to be achieved by the SHM technique the next topic is related to the choice of the distinct vibration-based methods for damage detection. Their basic premise is that damage significantly alters stiffness, mass or energy dissipation resulting in changes on the dynamic response of a system (FARRAR; SOHN, 2000; FARRAR; WORDEN, 2007). As discussed by Sohn and Farrar (2001), a extensive review of vibration-based damage identification methods which rely on detailed finite element modeling and/or modal properties of the structure was presented in Doebling et al. (1998). Moreover, some cases require data from the undamaged structure which is not always available. Although these methods are capable of reaching up to stage four of monitoring – *quantification of damage severity* – they were not effective in detecting early stage damage in practical applications.

On the other hand, a feasible way to overcome the drawbacks of the previous method is to perform damage detection employing statistical analysis of time series. An attractive advantage is the possibility to develop automated SHM techniques since only signal processing is performed and no intricate physical model is required (FARRAR; SOHN, 2000; SOHN et al., 2001; FUGATE et al., 2000; FASSOIS; SAKELLARIOU, 2007). Moreover, time series can be used to construct autoregressive models using well-known results from system identification and signal processing areas (SOHN et al., 2000; LU; GAO, 2005; SILVA et al., 2011). This approach provides advantages over traditional damage detection techniques (e.g. electromechanical impedance) since autoregressive models do not require domain transformation whose realization is dependent on important estimation parameters and on the frequency range adopted (SOHN et al., 2001; FASSOIS;

SAKELLARIOU, 2007; SILVA et al., 2008; FIGUEIREDO et al., 2011). Farrar and Sohn (2000) presented a useful guide to the understanding of the damage detection paradigm based on time series processing. In the previous work this process is divided in four stages:

1. Operational evaluation.
2. Data acquisition and cleansing.
3. Feature selection and data compression.
4. Statistical model development for feature discrimination.

The first topic is concerned with the characteristics and limitations of the SHM system including the operational and environmental conditions which the structure will be subjected. The second topic is related to the measurement system by the selection of sensors and their localization on the structure beside the eventual use of compensation procedures when data is measured under varying conditions. In such case the next topic, selection of signal features, has to be carefully performed since they are normally also sensitive to operational and environmental variability (SOHN, 2007). Finally, statistical models can be applied on the extracted signal features in order to evaluate the structural integrity. Additionally, feature discrimination provided by these models is crucial to separate or normalize the effects of other conditions on the dynamic behavior of a system from the effects of damage, such as load and temperature variations.

2.3 Damage Detection under Operational and Environmental Variability

As it can be noticed, all the four topics that compose SHM techniques based on time series analysis are somehow related to the varying conditions that the monitored structure will be subjected. However, the development of the second and the fourth part – *data aquisition and cleansing* and *statistical models*, respectively – directly deal with the strategies to overcome this issue (FIGUEIREDO et al., 2011). An example of how these varying conditions play an important role was verified in Sohn et al. (1999) in which the temperature variations during the tests caused the most expressive effects on the monitored parameters, completely masking the identification of damage.

2.3.1 *Compensation Procedures*

Compensation may be employed in an attempt to eliminate the influence of undesired effects in the early stage of damage detection helping the selection of adequate signal features (third step). Such strategy falls into two general classes (SOHN; FARRAR, 2001). The first approach is based on the parametrization of normal conditions of the structure obtained from the measurement of parameters related to varying operational and environmental conditions (e.g. load and temperature) besides vibration responses. This is useful in cases when such conditions produce the same effect as damage in the signal features. However, in some cases these measurements are a hard task thus, the second class of compensation has to be performed based on the selection of features exclusively sensitive to damage. In other words, the change produced in the chosen signal features is orthogonal to the changes caused by operational and environmental conditions (SOHN, 2007).

This fact is specially verified in electromechanical impedance signatures in which the overall effect of temperature variation is a combination of uniform horizontal and vertical translations (SUN et al., 1995). Park et al. (2003) state that, in general, the increase of temperature causes the decrease in magnitude of impedance and leftward shifting of the real part of electric impedance. On the other hand, as it can be verified in the work of Park et al. (2000), damage will significantly change the signature pattern, thus it can be detected. Bhalla et al. (2003) studied the components of simulated electromechanical impedance signatures to verify parts of the response with increased sensitivity to damage and reduced influence of temperature. With this separation an improved damage detection can be performed directly from these enhanced signatures.

Because information related to temperature can be extracted directly from electromechanical impedance signatures, the measurement of this parameter is unnecessary. Basically, unknown signals are correlated to a reference signal to provide the amount of translation for the compensation performed by inverse shifts. Sun et al. (1995) used the CCDM[1] between the baseline and unknown signatures to compensate frequency changes. Similarly, Park et al. (1999) performed a procedure employing a modified root mean square deviation metric which calculates the amount of horizontal shift to be compensated. Baptista et al. (2012) created a real-time data acquisition from multiple sensors based on the measuring system proposed in Baptista and Filho (2009) including compensation of temperature effects using CCDM. It was verified that temperature changes on impedance signature

[1] *Correlation coefficient deviation metric* – detailed in the next chapter.

show an approximately linear effect confirming that this effect can be compensated by a reverse horizontal shift. The CCDM was chosen due to its less susceptibility to variations in amplitude.

Temperature compensation is broadly used in Lamb wave techniques with the advantage of not requiring measurements of such parameter as well. Two procedures are commonly employed: optimal baseline selection (OBS) which compares a current time-trace to baseline time-traces measured at different temperatures to find the best match and; baseline signal stretch (BSS) that requires only one baseline time-trace which is modified to match the current time-trace.

As an example, Lu and Michaels (2005) employed both strategies to create a methodology for damage detection using diffuse ultrasonic waves in aluminum plates under temperature variations. A baseline OBS database was created by a collection of signals measured at specific temperatures covering the whole range experienced by the structure. After performing the optimum selection, BSS is carried to best match the monitored signal since the database cannot continuously represent every temperature within the range. Next, the presence of damage is evaluated by the computation of the normalized mean squared error between both signals. Thresholds and probabilities of detection are defined by the amount of signals to compose the baseline database.

The distinct characteristics of these two procedures were verified in many works with equal results. Wilcox et al. (2008) compared different strategies for temperature compensation and noted that time-domain stretch provides reasonable compensation for nondispersive signals under small temperature changes while OBS is suitable for large temperature variation. An similar approach was performed by Croxford et al. (2008) who tested various compensation strategies obtaining better achievements for OBS with numerical stretching or compressing. It was noted that OBS provides better results for nonuniform temperature changes which often happens in real applications. Finally, Croxford et al. (2010) found a reasonable temperature step of 1-2°C for this combined strategy. The authors state that these compensation methods are also applicable to environmental changes that result in isotropic change in wave velocity (e.g. hydrostatic pressure) whereas operational changes that cause anisotropic changes in velocity, such as the application of load in one direction, cannot be compensated remaining an open problem.

An approach analogous to OBS can be developed using autoregressive models, as carried by Sohn and Farrar (2001). In this work damage detection and localization are performed by the creation of a two-stage prediction model assuming that the prediction error of the autoregressive (AR) model is caused mainly by operational and environmental variability. This parameter is then used as the input of a autoregressive model with exogenous input (ARX) whose new prediction error is only damage sensitive. Reference ARX models are determined to create a database of coefficients to be used for the prediction of the new ARX models for unknown condition signals. The selection is based on the creation of an AR model for the test signal whose coefficients are compared to the collection of reference AR models to find the best match and to determine the respective ARX coefficients. One advantage regarding the computation of an autoregressive model for each analyzed condition is to enable the correlation of different types of damage to specific changes in the behavior of these coefficients (e.g. gradual loss of mass). The same approach can be associated to statistical models, which will be explained in the following topic, in order to improve damage detection (SOHN et al., 2001; SOHN et al., 2002).

2.3.2 *Statistical Models*

Statistical models have the capability to evaluate the effects of operational and environmental conditions on damage-sensitive features without requiring measurements of the former parameters nor physics-based models (FIGUEIREDO et al., 2011). The algorithms for statistical models can be divided into *supervised* and *unsupervised* learning. The first class refers to cases in which data from damaged and undamaged structures are available (e.g. group classification and regression analysis) while the second class is related to cases when data from the damaged structure is not available (e.g. outlier detection). Since in many situations it is impossible to obtain data from a similar damaged system, damage detection must be performed in an unsupervised learning mode (SOHN et al., 2000; FUGATE et al., 2000).

Therefore, the previous class of methods have proofed to be a suitable choice for damage detection in structures subjected to measurement variability (FUGATE et al., 2000; WORDEN et al., 2000). One first approach is to normalize the effects of operational end environmental conditions enhancing damage sensitivity on signal features. To do so, principal component analysis is commonly employed enabling data reduction as well. As an example, Sohn et al. (2000) applied principal component analysis on the coefficients of AR models considered to be damage sensitive resulting in data compression and in a maximized separation of features from the damaged and undamaged structure. The result is computed in statistical process control which has the advantage of being an automated continuous procedure. Park et al. (2008) created an on-board wireless system with enhanced analysis-capability provided by principal component analysis algorithm eliminating unwanted noises, such as temperature and humidity effects, through data compression. Then a root mean square deviation based index is calculated and the result is applied in a k-means clustering method. This procedure was compared to a simplified one based only on the previous index calculated from raw data evidencing the former method's improved detection capability. Lim et al. (2011) developed a robust monitoring technique based on data normalization using kernel principal component analysis to improve damage detection and minimize false-alarms caused by both load and temperature variations.

More elaborate methods are obtained with the use of statistical pattern recognition techniques to separate undesired effects from those related to damage. Silva et al. (2007) used a two step AR-ARX model created from vibration response measurements for linear prediction. Tests were carried in a simulated benchmark structure leading to many measurements that were compressed by principal component analysis in order to be applied in the model. Prediction errors were applied in a fuzzy clustering method separating undamaged to damaged conditions. Silva et al. (2008b) created a similar method firstly applying principal component analysis for data reduction from vibration signals measured in a three-story bookshelf structure to create as ARMA model. Next, prediction errors were used as structural-sensitive indices to test two fuzzy clustering methods – fuzzy c-means and Gustafson Kessel – evidencing the latter's better performance. Lopes Jr. et al. (2011) developed a fuzzy clustering method employing a combination of time and frequency domain features extracted from response signals capable of distinguishing temperature and load effects from those related to damage in an unsupervised way leading to an automated monitoring.

Figueiredo et al. (2011) tested four unsupervised machine learning algorithms (auto-associative neural network, factor analysis, Mahalanobis distance and singular value decomposition) for damage detection in a three story structure simulating operational and environmental variations by changing stiffness and mass conditions. Damage was simulated with the introduction of a bumper reproducing the effects of a crack. Again, no measurement of the sources of variability or physical models were required for the separation of effects. This work also evaluates the aptitude of such algorithms for embedded hardware which is a crucial issue for practical applications. Figueiredo et al. (2010) applied a nonlinear time series analysis based on a multivariate autoregressive model and hypothesis to monitor a structure similar to the one found in (FIGUEIREDO et al., 2011) under varying operational and environmental conditions. Such structure presents nonlinear behavior for some types of damage which often happens in real-world structures.

2.4 Damage Prognosis

Damage prognosis is the estimate of the remaining useful life of a damaged system (FARRAR, 2003). Damage will adversely affect its current and future performance occurring in two distinct time scales (FARRAR; WORDEN, 2007). As discussed before, damage can be nucleated at the material level and its propagation will depend upon the operational and environmental conditions leading to a catastrophic fault. On the other hand, damage can also occur on a much shorter scale of time due to discrete events, such as aircraft land, as presented by Inman et al. (2005). Because of the important dependence of damage on the operational and environmental conditions, the process of measuring such parameters for damage prognosis is known as usage monitoring (FARRAR; LIEVEN, 2007).

Damage prognosis capability is related to the evolution of simpler SHM techniques which only detect or localize damage (FARRAR; LIEVEN, 2007; WORDEN et al., 2007). This estimate relies on the creation of prediction models whose output together with usage monitoring information will attempt to forecast system performance (FARRAR; LIEVEN, 2007). The multidisciplinary nature of damage prognosis is evidenced by Chattopadhyay et al. (2013) whose report emphasize the mutual effort of material, sensor and data processing areas to create reliable prognosis strategies. The major interests for the development of methods to predict structural integrity are to improve the potential economic and life-safety benefits supplied by SHM.

As it can be noticed, the creation of predictive models is the main key for damage prognosis. After the current damage level is characterized by a SHM technique, it is evaluated in terms of failure mechanics and a damage law (KULKARNI; ACHENBACH, 2008). Since crack propagation is mainly caused by fatigue, different methods have been used to characterize and predict loading (LING; MAHADEVAN, 2012). A different approach is to attempt to model the structure's response under different levels of damage. This was performed by Albakri and Tarazaga (2014) who created electromechanical impedance signatures based on spectral element method. The prediction behavior of the model was verified by subsequent reductions in the stiffness of the modeled structure beside changes in the damage width and location. Another approach is to use statistical models to track changes in the structural condition.

On the other hand, it is possible to develop prognosis strategies without the need of intricate physical model. This fact was verified by SILVA et al. (2008) whose work dealt with the modeling of electromechanical impedance signatures associated to statistical process control for a reliable damage detection. It was observed that such processing evidenced a behaviour trend of the damage identification parameters enabling the quantification of damage present in the structure. Similarly, Pavlopoulou et al. (2013) used Lamb wave excitation to monitor composite panels under different loading conditions and tested outlier analysis, principal component analysis and nonlinear principal component analysis. All these models successfully represented the structural status confirming their aptitude to track structural integrity.

2.5 Conclusion

This chapter presented a succinct review of damage detection methods under the influence of operational and environmental variability and the capabilities of damage prognosis techniques were investigated. Thus the main conclusions are:

- Operational and environmental conditions affect dynamic properties of a structure leading to false damage diagnosis;
- A straightforward but reliable damage detection method can be developed based on statistical analysis models;
- Unsupervised learning methods are preferred for real-world applications since data from the undamaged structure is often unavailable;
- Damage prognosis is the evolution of SHM techniques since it can optimize the useful life of a system.

The review also demonstrates a new trend regarding the use of autoregressive models for SHM purposes employing well-known results from system identification and signal processing areas. Because such models are basically discrete filters, they do not require a great processing capability enabling their applicability in on-board wireless hardware. Also, they can be easily associated to statistical pattern recognition techniques to improve damage detection even under operational and environmental variability. Lastly, this approach can be associated to damage prognosis strategies in order to forecast the structure's future behavior.

3 Damage Detection in Composite Materials Considering Loading Effect

This chapter presents the development of a damage detection technique for a composite plate under series of loading. By using measured response signals, a reference AR model is identified and the separation of effects is performed by a fuzzy clustering method, as outlined in figure 1.

Figure 1 – Overview of the effect separation procedure.

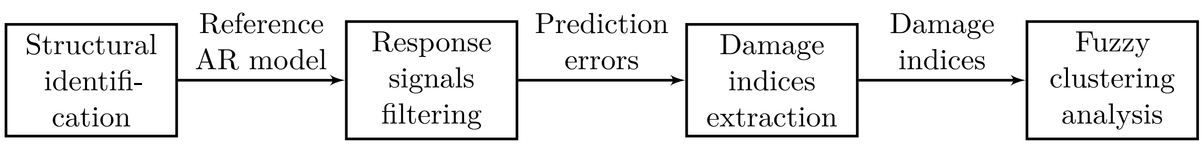

Source: Created by the author.

3.1 Experimental Setup

The following experimental tests were performed in Stanford University, Department of Aeronautics & Astronautics – Structures and Composites Laboratory, by Professor Dr. Vicente Lopes Júnior on a composite structure provided by NASA. The data from this test was already processed in Lopes Jr and Chang (2012) showing satisfactory separation of effects with the use of artificial neural network. The aim of this experiment is to use a Lamb wave based method to study the behavior of a structure through a series of loads. Sensor measurements were taken through two SMART® piezoelectric (PZT) sensor patches bonded to the surface of a thin rectangular composite plate as seen in figure 2. Each sensor has six PZT transducers which can act as both actuators and sensors. A pitch catch measurement mode was chosen so the top layer was arbitrary set to excite the structure (actuators) while the bottom one was used as sensors (figure 2(a)).

Data acquisition was performed by Acellent® acquisition board and controlled by

ACESS® software with a sampling rate of 12 MHz[1]. The excitation signal chosen was a five peak Gaussian tone-burst with actuation frequency of 300 kHz. This frequency generates a S0 packet, with an acceptable level of dispersion (figure 3(c)), which is sensitive to the kind of damage tested, proven by many theoretical and experimental works (TAN et al., 1995; LEMISTRE; BALAGEAS, 2001; TOYAMA; TAKATSUBO, 2004; HU et al., 2008). Experimental signals for the undamaged structure (reference condition) are shown in figure 3(a)-(b). Figure 4 shows response signals for different conditions of the structure in the time interval from 55 to 75 μsec in which the S0 packet is located.

Figure 2 – Composite structure coupled with two Smart® PZT sensor patches.

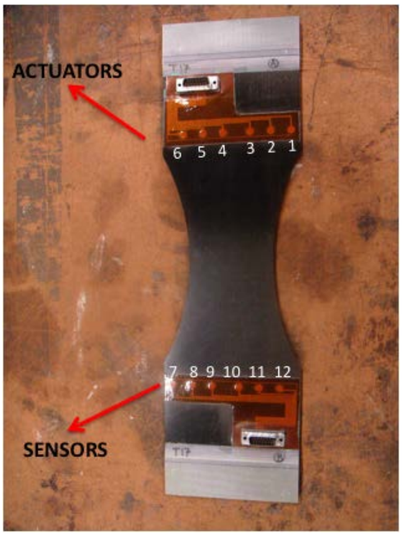

(a) Actuators and sensors in detail.

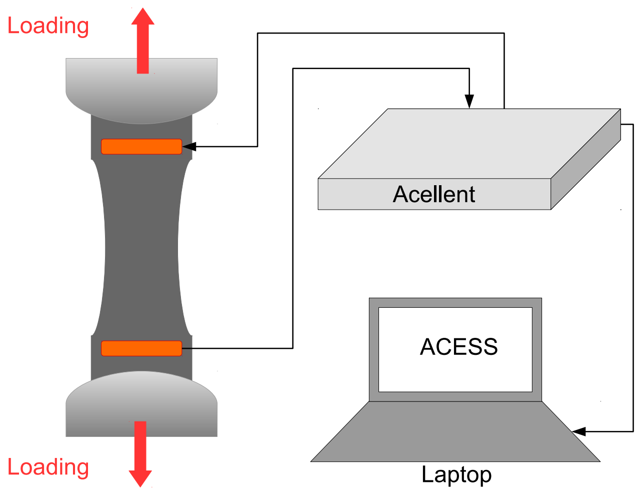

(b) Schematic representation of the composite structure attached to the MTS.

Source: (a) Lopes Jr and Chang (2012); (b) Created by the author.

Several sets of experiments were performed to collect data from different load conditions. Although all available paths have been measured, only path 3-9 was used in order to minimize possible reflections caused by corners which could affect the following methodology for damage detection. The loading series were applied through a MTS®[2] in three different days (figure 2(b)). In the first day the load ranged from 0 to 4.0 kip[3], as shown in table 1, column 1 and 2. After these tests, X-ray showed that there was no damage in the structure. In the second day, the load ranged from 0 to 7.0 kip, column 3 and 4. Initial delamination began in approximately 5.0 kip. The last set of tests was carried out until the rupture, column 5 and 6. The rupture occurred in approximately 10.8 kip.

---

[1]More information about the acquisition softwre at: http://www.acellent.com/blog1/products/software/

[2]*Material Test System* – equipment capable of applying controlled levels of load and/or temperature.

[3]The use of a non International System of Units unit is due to equipment limitation (1 kip = 4450 N).

Figure 3 – Reference signals and dispersion curves for the composite structure.

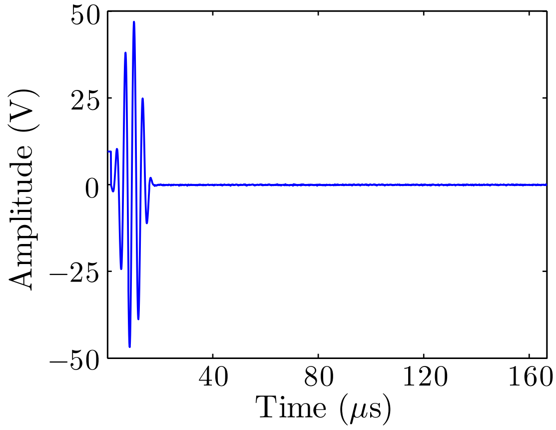

(a) Input signal for the undamaged structure.

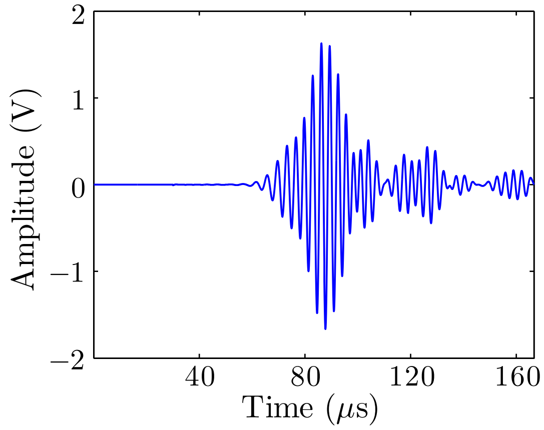

(b) Output signal for the undamaged structure.

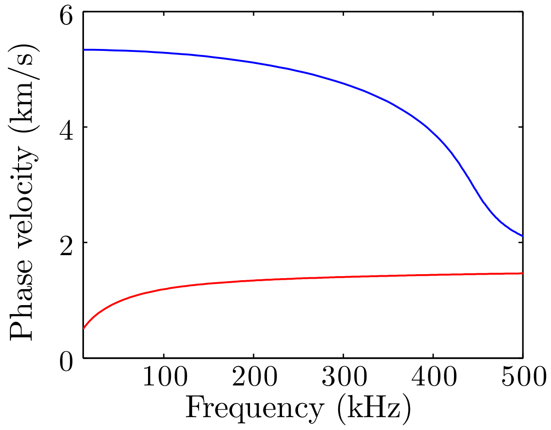

(c) Dispersion curves for the composite coupond (—— S0 packet, —— A0 packet).

Source: Created by the author.

Figure 4 – Response signals under loading effect.

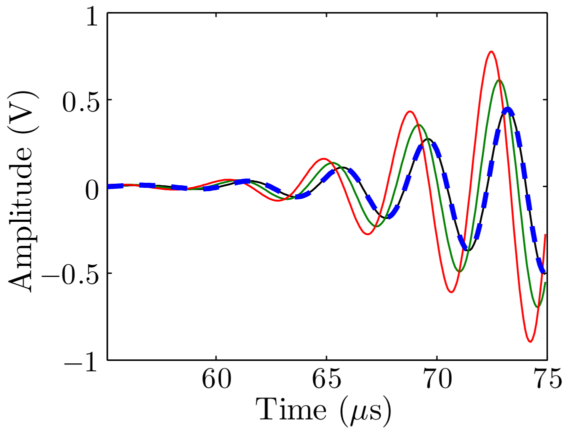

(a) Signals for the first loading series (—— test 1, —— test 5, —— test 9, – – test 10).

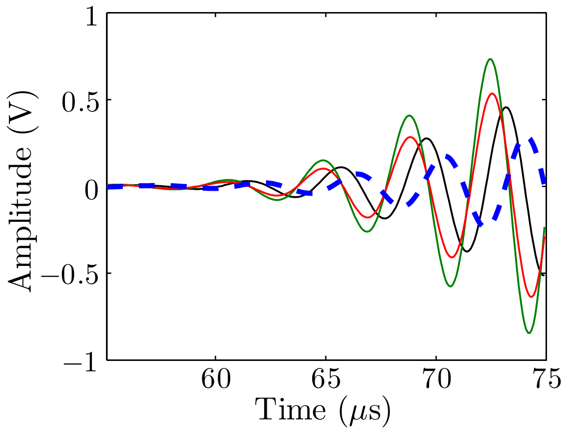

(b) Signals for the second loading series (—— test 11, —— test 15, —— test 19, – – test 22).

Source: Created by the author.

Table 1 – Test conditions (highlighted cells referring to unloaded condition).

Test Number	Load (kip)	Test Number	Load (kip)	Test Number	Load (kip)
1	**0**	**11**	**0**	**23**	**0**
2	0.5	12	1.0	24	1.0
3	1.0	13	2.0	25	2.0
4	1.5	14	3.0	26	3.0
5	2.0	15	4.0	27	4.0
6	2.5	16	4.5	28	5.0
7	3.0	17	5.0	29	6.0
8	3.5	18	5.5	30	7.0
9	4.0	19	6.0	31	7.5
10	**0**	20	6.5	32	8.0
		21	7.0	33	8.5
		22	**0**	34	9.0
				35	9.5
				36	10.0
				37	10.5

Source: Created by the author.

3.2 Extraction of Damage Indices

The ability to segregate data relies on the signal features which are extracted by damage indices. Thus, the chosen indices must provide enough information making possible the separation of the distinct effects that the structure is subjected. This work combines information obtained through time and frequency domain indices. Initially an AR model is created in order to reproduce the structure's response for the reference (undamaged) condition[4]:

$$A(q)y_{ref}(k) = e_{y_{ref}}(k) \tag{1}$$

where $y_{ref}(k)$ is the estimated response signal as a function of the discrete samples k and $A(q)$ is a polynomial identified for the reference condition in order to monitory unknown condition signals. The previous parameter is a function of the shift operator q whose of order n_a is obtained by the computation of the Akaike's information criterion (AIC) leading to a suitable value of 10. Then the model was validated with a certification signal – measurement 10 – with the same reference conditions (table 1). Certification was successful since an excellent fit percentage of 99.9% was obtained with the direct comparison of both signals (figure 5(a)). Additionally, an adequate level of residues in the response was

[4]See APPENDIX B for more information about the estimation and certification of autoregressive models.

verified with the calculation of the autocorrelation function (ACF) converging to a 10% confidence interval as the lags increase which ensures the model's ability to reproduce the structure's behavior (figure 5(b)).

Figure 5 – Validation of the reference AR model.

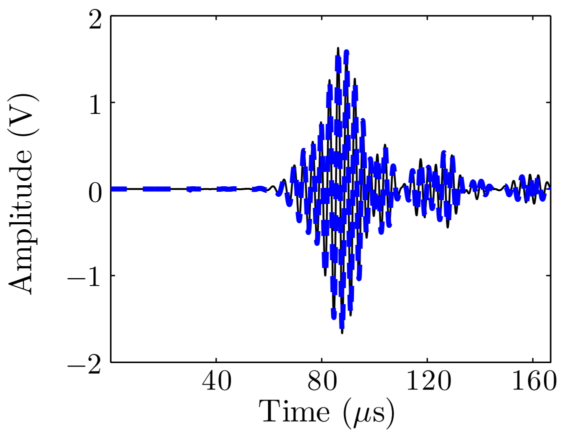

(a) Direct comparison between the certification signal (solid black line ——) and the adjusted signal (dashed blue line – –) with a fit percentage of 99.9.

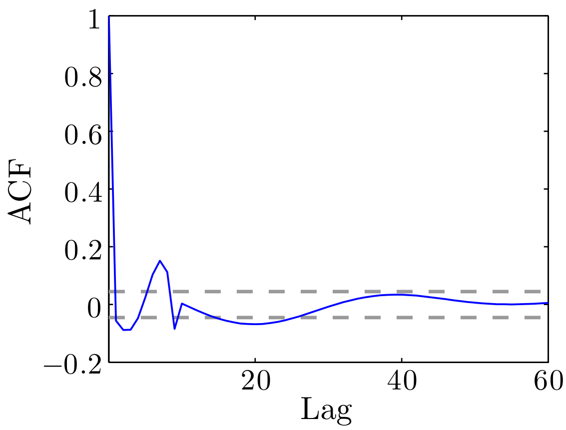

(b) Residue evaluation of adjusted response converging to the confidence interval of 10% as the past samples (lags) increase.

Source: Created by the author.

The prediction error $e(k)$ is related to the amount of the original response which is not represented by the model. It is important to note that despite of the ideal random behavior expected for the prediction error to ensure a good system's identification, in the present processing this parameter showed a deterministic behavior very similar to the response signals (figure 6). This was intentionally done so all effects acting on the structure besides load and damage were accounted in the model enabling the damage indices to be extracted directly from this parameter.

It is known that the change of the wave propagation is directly associated to material alterations due to varying operational and environmental conditions and/or the presence of damage[5]. Thus, it is possible to observe that the prediction errors suffered a leftward shift and amplification with the increase of tensile load. Also, the interruption of this pattern is verified between tests 15-19. This abrupt behavior change indicated that the handling of measurement variability sources could be performed by the application of a statistical model for the separation of effects without requiring any compensation procedures[6]. Thereby, the structural investigation was carried by the extraction of damage indices.

[5]See APPENDIX A for more information about wave propagation.
[6]A review of compensation strategies was presented in chapter 2

Figure 6 – Prediction errors.

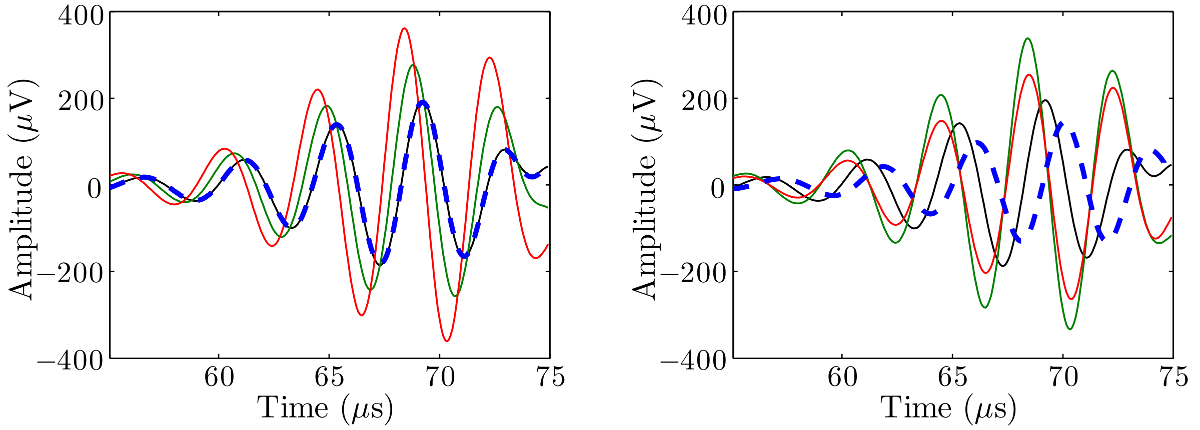

(a) Signals for the first loading series (——— test 1, ——— test 5, ——— test 9, – – test 10).

(b) Signals for the second loading series (——— test 11, ——— test 15, ——— test 19, – – test 22).

Source: Created by the author.

Firstly, the γ index was applied on the prediction errors (LU; GAO, 2005):

$$\gamma = \frac{\sigma(e_{unk})}{\sigma(e_{ref})} \tag{2}$$

where $\sigma(*)$ is the standard deviation operator, e_{ref} and e_{unk} are the prediction errors for the reference and unknown conditions, respectively. Because this index is based on the standard deviation it is more sensitive to variations in amplitude. Next, the cross correlation deviation metric (CCDM) was calculated using the prediction errors as well (GIURGIUTIU, 2002):

$$CCDM = 1 - \left| \frac{\sum_{k=1}^{N}(e_{k,ref} - \bar{e}_{ref})(e_{k,unk} - \bar{e}_{unk})}{\sqrt{\sum_{k=1}^{N}(e_{k,ref} - \bar{e}_{ref})^2}\sqrt{\sum_{k=1}^{N}(e_{k,unk} - \bar{e}_{unk})^2}} \right| \tag{3}$$

where k is referred to discrete samples, N indicates the range of values for the calculations. As discussed in chapter 2, CCDM is less sensitive to variations in amplitude but capable of detecting phase shifts.

Besides the time domain analysis performed, a time-frequency domain analysis is carried by the extraction of the short-time Fourier transform (STFT) whose matrix provides the energy map[7]. Its decomposition using singular value decomposition generates diagonal matrix Σ which is sensitive to structural alteration. The trace index is obtained through

[7]See APPENDIX C for more information about time-frequency analysis and the calculation of the trace index.

the sum of its diagonal terms:

$$Trace = \sum_{i=1}^{N} \mathbf{\Sigma}_{ii} \tag{4}$$

where $\mathbf{\Sigma}_{ii}$ are the diagonal terms of matrix $\mathbf{\Sigma}$. These three indices were normalized in relation of their greatest value to generate a value range between 1 and -1 as presented in figure 7.

Figure 7 – Damage indices calculated for the clustering method ($*$ – γ index, $\diamond$ – CCDM, $\square$ – trace).

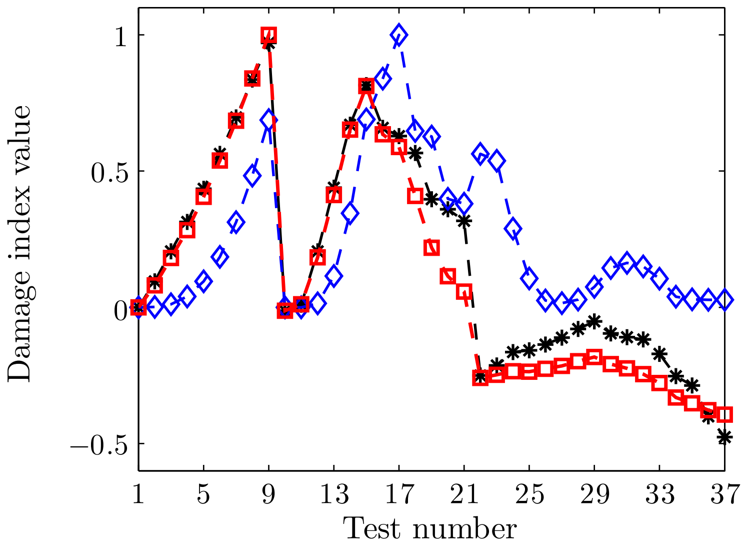

Source: Created by the author.

3.3 Cluster Analysis Results

The three damage indices calculated for the 37 load conditions, presented in table 1, were used in the separation performed by fuzzy c-means[8] (figure 7) which is explained in APPENDIX D. The number of clusters is an unknown information, but it is crucial to the adequate classification. In the present procedure, the number of clusters was set as five – undamaged or reference condition, two levels of load and two levels of damage – mainly because of the knowledge of the effects that acted on the structure throughout the experiment. This choice can be a issue in cases where not all the sources of measurement variability are known.

The result of the fuzzy clustering classification is showed in figure 8 in which it is possible to see that the representation of effects was well described. Due to the experimental

[8] See APPENDIX D for more information about fuzzy clustering analysis.

configuration, it is expected that the structure goes from a reference condition to increased load conditions. Despite the fact that loads up to 1.5 kip were classified into the reference cluster, the fuzzy clustering method confirmed no damage was imposed to the structure on the first load series, as seen in figure 9. Besides, the increasing load effect discussed before was verified. Damage was detected by the X-ray on the second load series around measurement 17 (5.0 kip), which is evidenced by the close classification at measurement 19 (6.0 kip). This fact confirms the accuracy of fuzzy c-means for damage detection.

Figure 8 – Three dimensional distribution of damage indices with cluster division (○ – class 1, △ – class 2, ◊ – class 3, ∗ – class 4, □ – class 5, × – class center).

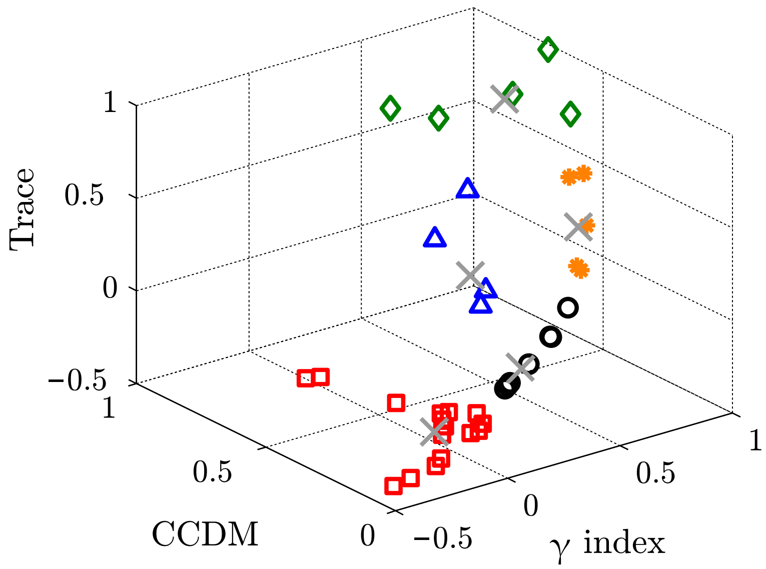

Source: Created by the author.

Moreover, since damage permanently changes the structure, no other undamaged condition is verified after damage is first detected (figure 9). Also, the cumulative effect of damage is captured as the classification goes from low damage to high damage definitively. Finally, imprecision in the classification can be related to the limited amount of data and operational condition diversity.

3.4 Conclusion

This experimental and processing procedure presented a strategy to distinguish the signal variation caused by loading from those caused by damage in order to avoid false diagnosis occurrence. This approach is based on the computation of damage indices on prediction errors provided by a reference AR model. The use of autoregressive models is justified by their simple implementation and certification. Besides the two indices based on time domain analysis, spectrogram parameters are used in a fuzzy clustering method as well. This procedure successfully separated load effects from damage effects resulting in a reliable damage detection. Thus, the proposed approach is a robust unsupervised damage detection method that can be used in applications in which operational and environmental conditions play an important issue.

Figure 9 – Percentage results of fuzzy *c*-means classification: reference (Ref), low load (LL), high load (HL), low damage (LD) and, high damage (HD).

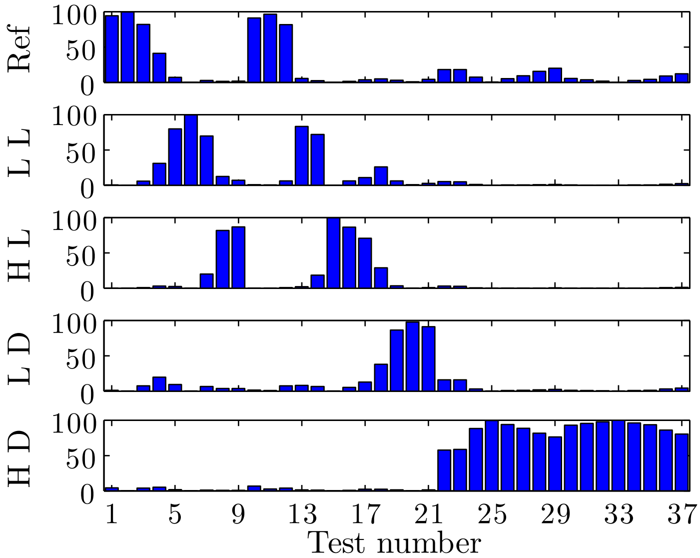

Source: Created by the author.

Although fuzzy clustering is considered to be an unsupervised method, it is important to highlight that the separation is performed after all data is collected. Besides, considering that an actual application requires a continuously monitoring, the separation of effects has to be done with a limited amount of information. In other words, only the reference condition is well characterized and other conditions (operational and environmental or damage) are to be identified through the monitoring. Thereby, the present technique is suitable for behavior mapping of the structure prior to the use of an identical component in a real world application as long as the varying conditions remain the same.

4 Damage Prognosis based on Coefficient Extrapolation

In this chapter a damage detection procedure with statistical confidence is carried using statistical process control. Also, a damage prognosis strategy is developed in order to forecast damage evolution in an aluminum plate subjected to a localized progressive mass loss. The prediction is based on the extrapolation of coefficients from identified structural conditions to create theoretical predictive models. This procedure is outlined in figure 10.

Figure 10 – Overview of damage detection associated to prognosis procedure.

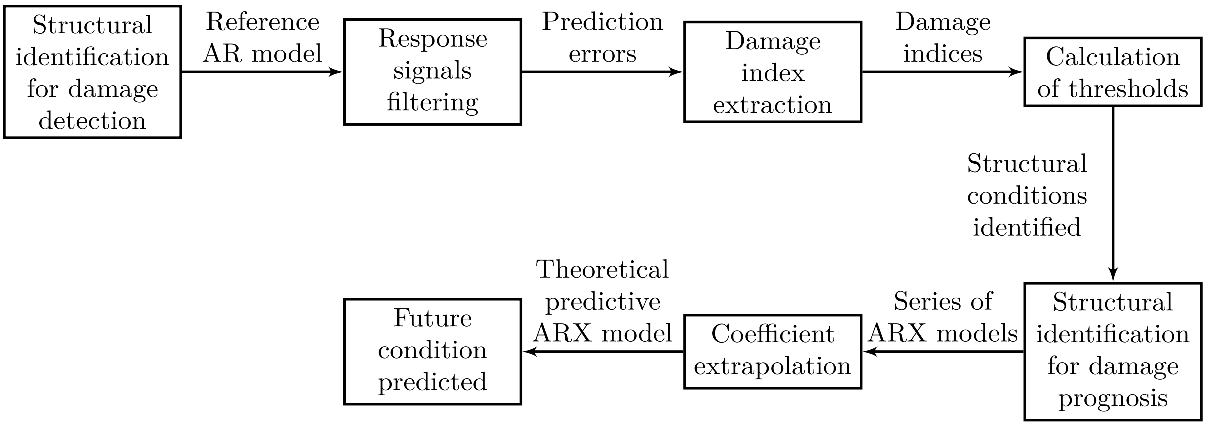

Source: Created by the author.

4.1 Experimental Setup

The present experimental tests were carried in CPqD[1], Laboratory of Mechanical Tests, on a 1.6 mm thick aluminum plate coupled with six piezoelectric (PZT) patches (figure 11(a)). The structure was clamped at both ends in order to reduce measurement interference and kept at controlled room temperature (23 ± 3 °C), as showed in figures 11(b) and 12. A pitch-catch measurement mode was chosen with PZT 5 as actuator and PZT 2 as sensor. Data generation and acquisition was performed by a National

[1] *Centro de Pesquisa e Desenvolvimento em Telecomunicações* – http://www.cpqd.com.br.

Instruments® PXI module and controlled by LabVIEW® software with a sampling rate of 10 MHz and an acquisition time window of 1.5 ms. The structure was excited by a five peak Gaussian tone-burst with 10 V_{pp} of amplitude and actuation frequency of 150 kHz to guarantee damage detectability[2] (figure 13(a)-(b)). This frequency generates an A0 packet[3] of 930 m/s (figure 13(c)) with around 6 mm of wavelength which is located at the time window from 200 to 230 μs.

Figure 11 – Aluminum plate and the generation and acquisition system.

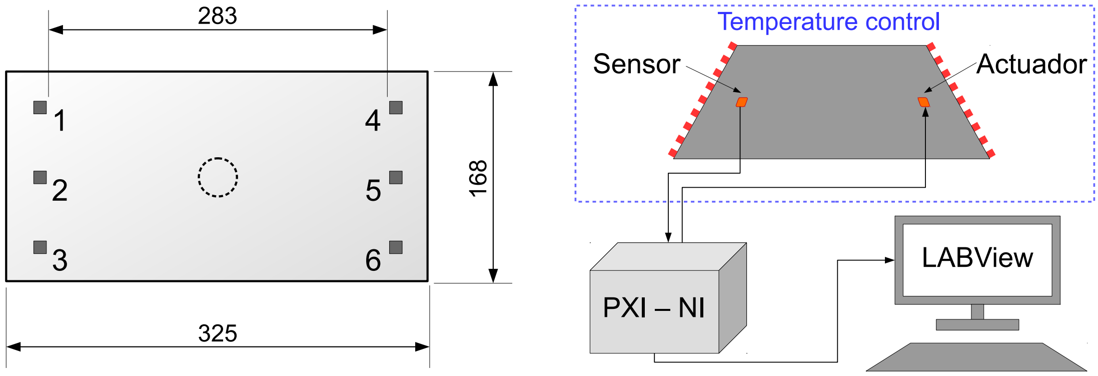

(a) Aluminum plate and its dimensions (dashed circle indicating damage location).

(b) Schematic representation of the aluminum plate.

Source: Created by the author.

Figure 12 – Experimental setup for damage prognosis.

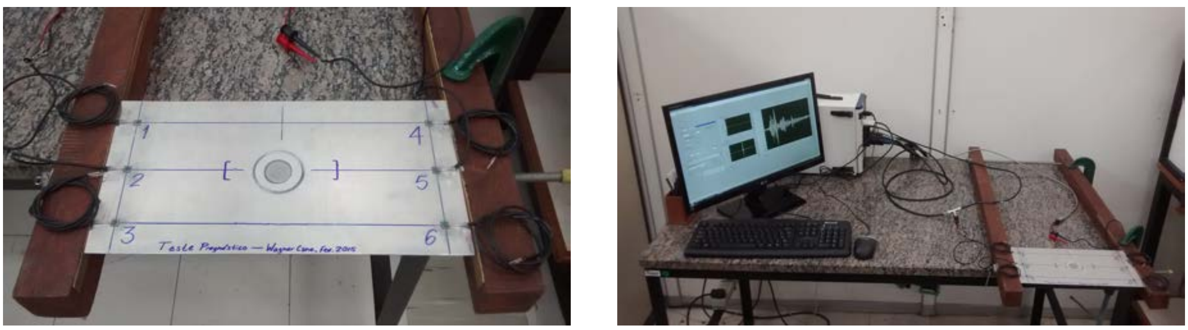

(a) Aluminum plate coupled with six Piezo Systems® PZT sensor patches.

(b) Data generation and aquisition system and plate support.

Source: Created by the author.

Two series of 10 signals were measured in distinct periods for each case studied for repeatability evaluation, as presented in table 2, with each acquired signal being a mean

[2]See APPENDIX A for more information about wave propagation.

[3]This choice is explained by the effective thickness reduction caused by the kind of damage tested which alters the frequency-thickness product leading to phase velocity reduction of packet A0, as observed in figure 13(c). Besides, it is intuitive that geometric alterations characterized by the term h (plate thickness) will result in propagation changes governed by equation 11 – APPENDIX A.

of 10 signals. The response signals were normalized to produce zero mean and unitary standard deviation as a requirement for the following statistical methodology developed for damage detection (figure 14).

Figure 13 – Reference signals and dispersion curves for the aluminum plate.

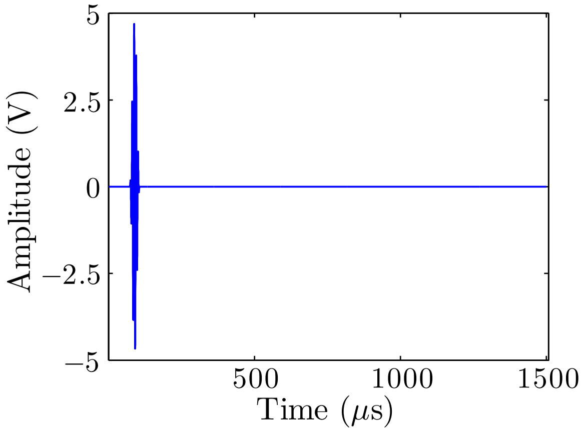

(a) Input signal for the undamaged structure.

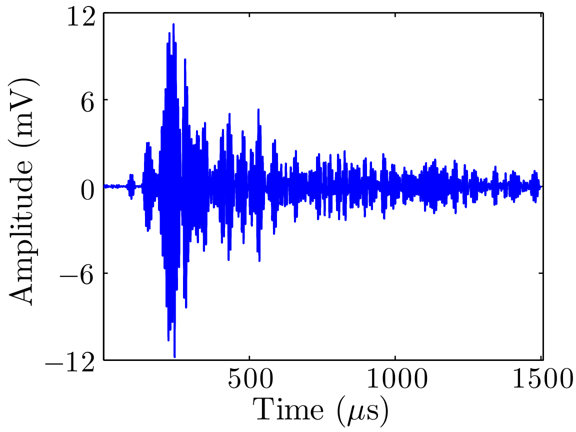

(b) Output signal for the undamaged structure.

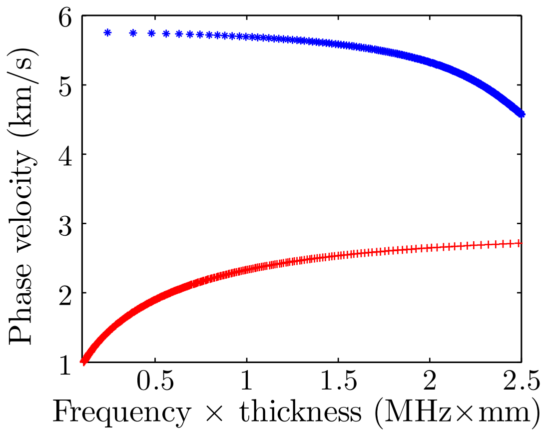

(c) Dispersion curves for the aluminum: ∗ – S0 mode; + – A0 mode.

Source: Created by the author.

Table 2 – Sequence of measurements.

Condition tested	Test number	Damage depth (mm)	Thickness reduction (%)
Reference	1 - 20	0	0
Damage 1	21 - 40	0.10	6.25
Damage 2	41 - 60	0.20	12.50
Damage 3	61 - 80	0.30	18.75
Damage 4	81 - 100	0.40	25.00

Source: Created by the author.

Damage was simulated through subsequent electrolytic polishing procedures resulting in localized mass loss of 22 mm in diameter taking into account the rule that this dimension must be greater than half size of the wavelength generated (LEE; STASZEWSKI, 2003). This procedure was carried in the same face as the PZTs were bonded to the plate in an attempt to reproduce the effects of corrosion, which often affects aircraft structures and is hard to detect in inaccessible areas (figure 15).

Figure 14 – Normalized response signals in the time window from 200 to 230 μs corresponding to the first antisymmetric wave mode – A0 (— — test number 1, —— test number 21, —— test number 41, — — test number 61, —— test number 81).

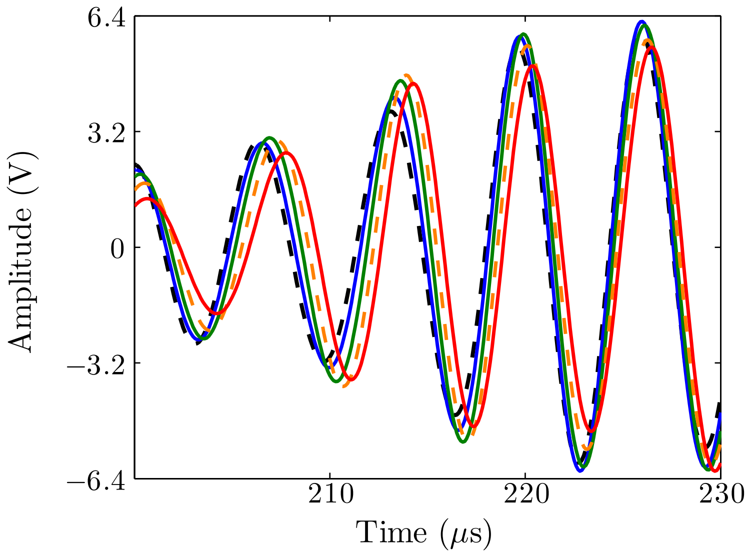

Source: Created by the author.

4.2 Damage Detection

The first of the two step identification was based on the estimation of a *reference AR model* to provide a parametrization of the undamaged structural condition[4]. In this sense, model identification and validation were performed using the first two signal responses, respectively (test numbers 1-2), since at this point the structure was considered to be undamaged (reference state). The model order determination was guided by the AIC index but also to ensure that the prediction errors would be able to carry information about damage, enabling the detection (figure 16). Thus, to meet such requirements, a suitable value for the reference model order was 2, leading to a satisfactory validation presented in figure 17.

[4]See APPENDIX B for mode information about the identification and validation of autoregressive models.

Figure 15 – Apparatus for the creation of a controlled damage with progressive depth.

(a) Buehler® Electromet 4 electrolytic polisher composed of an electric circuit and an acid solution pump capable to produce controlled mass loss.

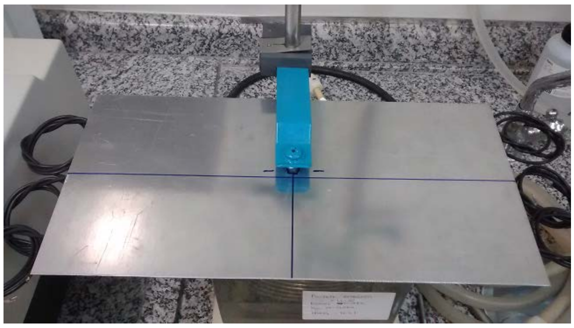

(b) Structure under electrolytic polishing .

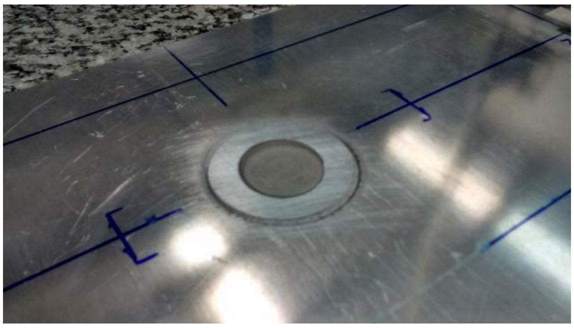

(c) Resulting localized damage in detail to simulate corrosion.

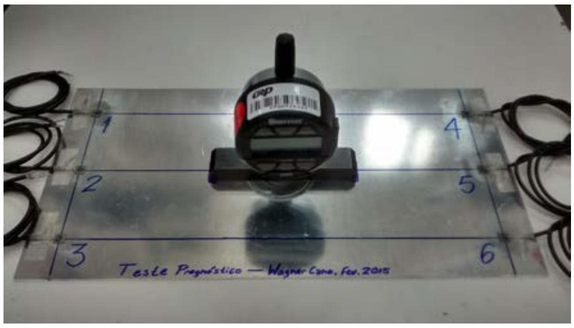

(d) Damage depth measurement by a Starret® 2900 electronic indicator.

Source: Created by the author.

Figure 16 – AIC index and prediction errors of the reference AR model for damage detection.

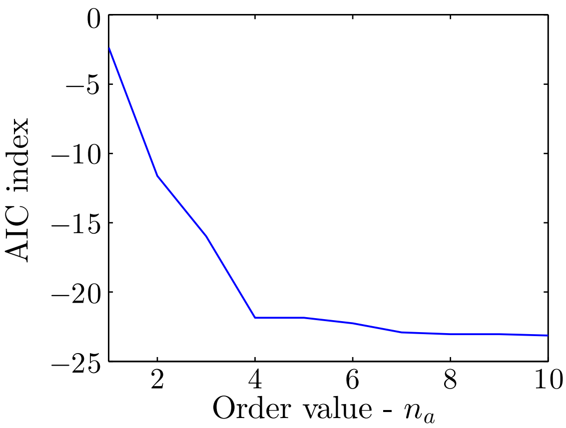

(a) AIC index for the reference AR model.

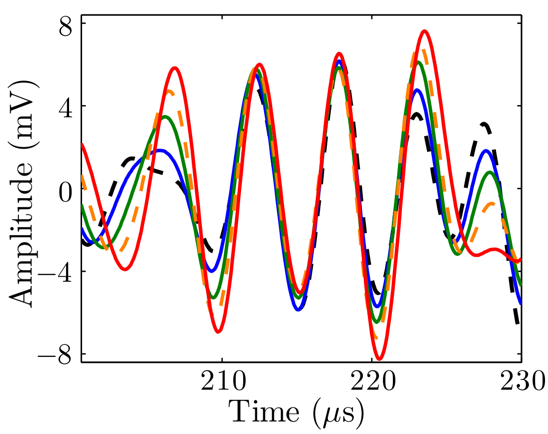

(b) Prediction errors (— — test number 1, —— test number 21, —— test number 41, — — test number 61, —— test number 81).

Source: Created by the author.

The γ index was used as the damage index due to its better sensitivity to variations in amplitude since data dispersion is expected in the prediction errors when response signals of damaged conditions are filtered by the reference AR model. This index is defined as (LU; GAO, 2005):

$$\gamma_N = \frac{\sigma(e_N)}{\sigma(e_{N_{ref}})} \tag{5}$$

where N is the test number and the subscript ref refers to the position of the reference indices with $N_{ref} = 1, 2, 3, \cdots, 10$ in this case generating 10 indices per test number, as presented in figure 18(a).

Figure 17 – Validation of the reference AR model for damage detection.

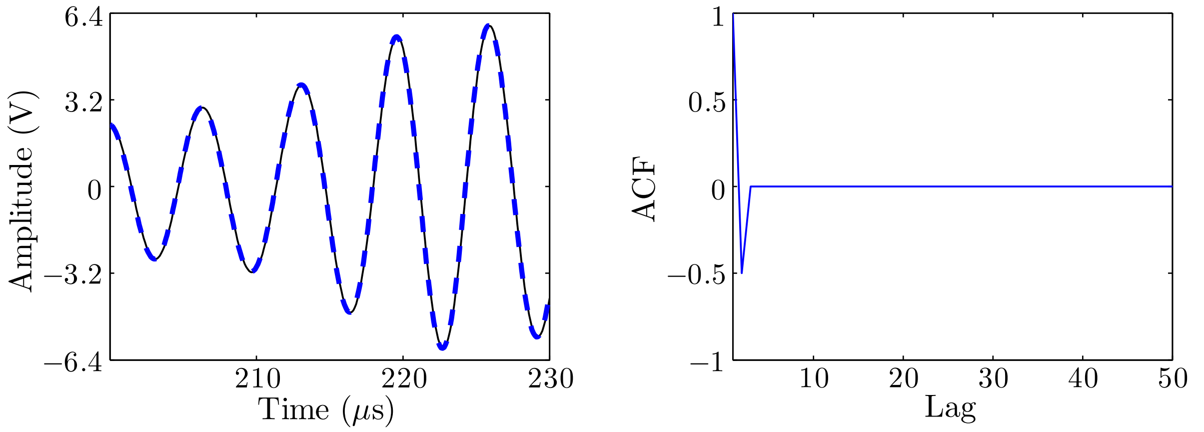

(a) Direct comparison between the certification signal (solid black line ———) and the adjusted signal (dashed blue line ‒ ‒) with a fit percentage of 99.9.

(b) Residue evaluation of adjusted response converging to the confidence interval of 10% as the past samples (lags) increase.

Source: Created by the author.

The thresholds for damage occurrence are defined by the computation of the control chart X-bar using the mean γ index value denoted by $\bar{\gamma}$ (figure 18(b)). To do so, only first 10 indices calculated were employed – the other 10 signals (test numbers 11-20 of the reference condition, for example) were kept to verify measurement variability and the occurrence of false indications of damage. The first step is the rearrangement of the indices in m subgroups of size n, normally chosen to be 4 or 5 (MONTGOMERY, 1996):

$$[\bar{\gamma}]_{i,j} = \begin{matrix} \bar{\gamma}_{1,1} & \bar{\gamma}_{1,2} & \cdots & \bar{\gamma}_{1,n} \\ \bar{\gamma}_{2,1} & \bar{\gamma}_{2,2} & \cdots & \bar{\gamma}_{2,n} \\ \vdots & \vdots & \ddots & \vdots \\ \bar{\gamma}_{m,1} & \bar{\gamma}_{m,2} & \cdots & \bar{\gamma}_{m,n} \end{matrix} \tag{6}$$

The motivation for the use of subgroups is that the distribution of the subgroup mean can be reasonable approximated by a normal distribution as a result of the central limit theorem (SOHN et al., 2000). Thus, the mean and the standard deviation of each subgroup is calculated for $i = 1, 2, \cdots, m$:

$$\overline{X}_i = \mu(\bar{\gamma}_{i,j}) \qquad S_i = \sigma(\bar{\gamma}_{i,j}) \tag{7}$$

with $\mu(*)$ and $\sigma(*)$ being mean and standard deviation, respectively. Next, the central line (CL) is obtained with the following expression:

$$CL = \mu(\overline{X}_i) \tag{8}$$

Since data dispersion is expected for damaged conditions, only the upper control limit (UCL) is used as the threshold for damage detection:

$$UCL = CL + Z_{\alpha/2}\frac{S}{\sqrt{n}} \tag{9}$$

where $S = \mu(S_i)$. Due to measurement variability, the number of subgroups n was defined as 2 resulting in a subgroups of 5 elements. The term $Z_{\alpha/2}$ is the point in a normal distribution of zero mean and unitary standard deviation such that $P(z > Z_{\alpha/2}) = \alpha/2$. In the present work a confidence interval of 99.73% was chosen leading to $Z_{\alpha/2} = 3$. Therewith, damage is detected when damage index value becomes greater than the threshold.

Figure 18 – Damage indices for the reference condition.

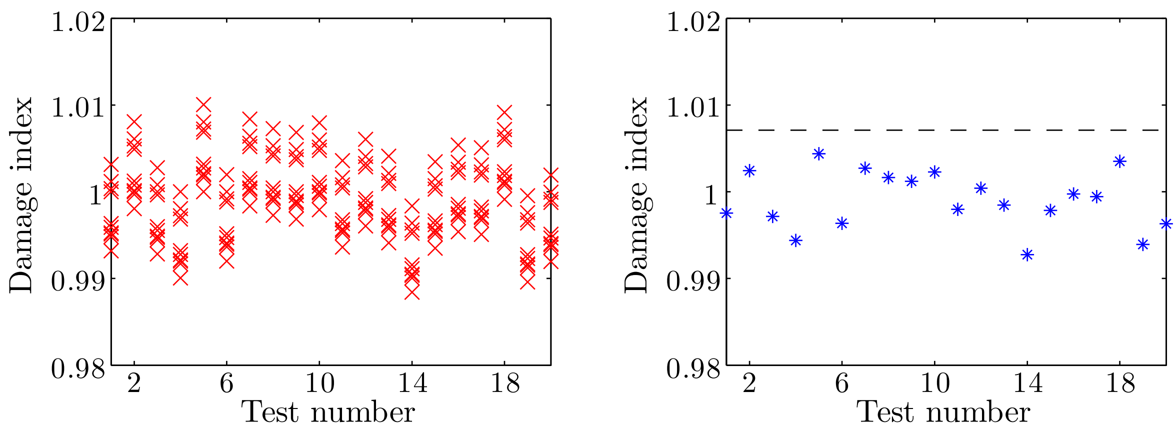

(a) 10 γ inidces obtained for each test number.

(b) Mean γ indices ($*$) calculated for each test number and the respective threshold (— —).

Source: Created by the author.

When such fact is observed, a new threshold value is defined by equation (9) to enable the detection of more severe damage. Figure 19 presents the damage indices computed for all signals measured whose behavior demonstrated the expected increase of data dispersion as damage became more severe. It is possible to obverse, for example, that damage index of test number 21 is located above the first threshold. At this moment damage is detected and a new threshold is obtained with the damage indices calculated with response signals from test numbers 21-30. These two identified conditions could enable the prediction of a third one as long as damage location and mass loss progression remain the same employing an adequate prognosis methodology.

Figure 19 – Damage indices (γ index) and thresholds for damage detection.

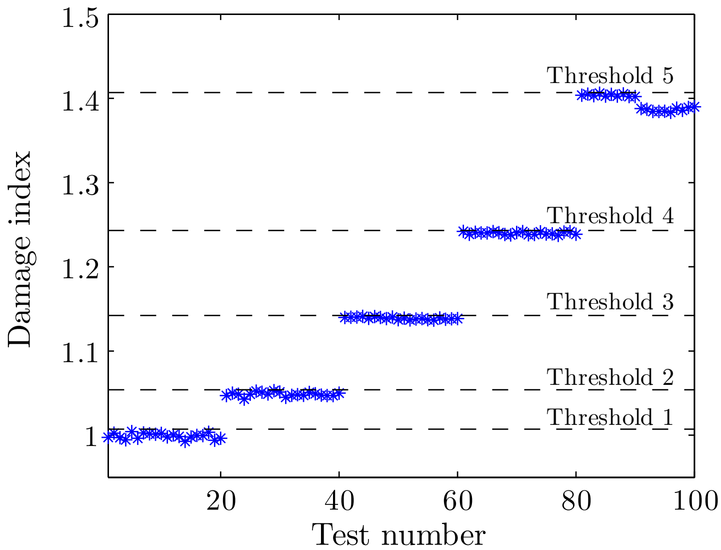

Source: Created by the author.

4.3 Damage Prognosis

As discussed before, the *reference AR model* for damage was estimated so the resulting prediction errors were able to carry information about damage progression. Similarly, the second step of the proposed structural identification is based on the modeling of response signals using autoregressive models with exognous inputs (ARX). This choice was guided due to the subtle changes verified in the response signals for the different conditions tested – predominantly phase shifts. Since ARX models consider the influence of the input signal to estimate the system´s output signal[5], they are believed to better capture structural behavior exclusively for the condition they were created. This premise is crucial to ensure an adequate and unique identification of each structural condition tested enabling the prognosis of the structure´s future behavior by coefficient extrapolation.

[5]The same results presented for the AR model in the APPENDIX B can be derived for the ARX model modifying the simplification that generated equation (13) with $B(q) \neq 1$

The following procedure aims to forecast the structure's behavior for a future condition taking into account past modeled conditions. Firstly, the input signal and the A0 packet of the response signals of test numbers 1-10 were used to create the first series of *structural identification models*. Model validation was performed with signals from test number 11-20, so model 1 was validated with signals from test number 11 and so on. New of these series are created for the other damaged conditions detected as well, similarly to what was performed for the thresholds[6].

The compromise to generate structural identification models "dedicated" only to the structural condition that they were created led to a order choice of $n_a = 4$ and $n_b = 3$. The validation of the first ARX model created and validated with signals from test 1 and 11, respectively, is presented in figure 20 with an excellent fit percentage higher than 99% and a minimum level of residues in the response. All other structural identification models obtained for reference and damaged conditions presented similar results so their validation was omitted. Such capability was evaluated by the data dispersion in the prediction errors since this parameter should be minimized when both model and signals are related to the same condition, as discussed before. Each group of 10 structural identification models generated a set of prediction errors whose standard deviation was calculated. Their mean value and dispersion is presented in figure 21 evidencing the desired characteristic.

Figure 20 – Validation of the first structural identification model for the reference condition.

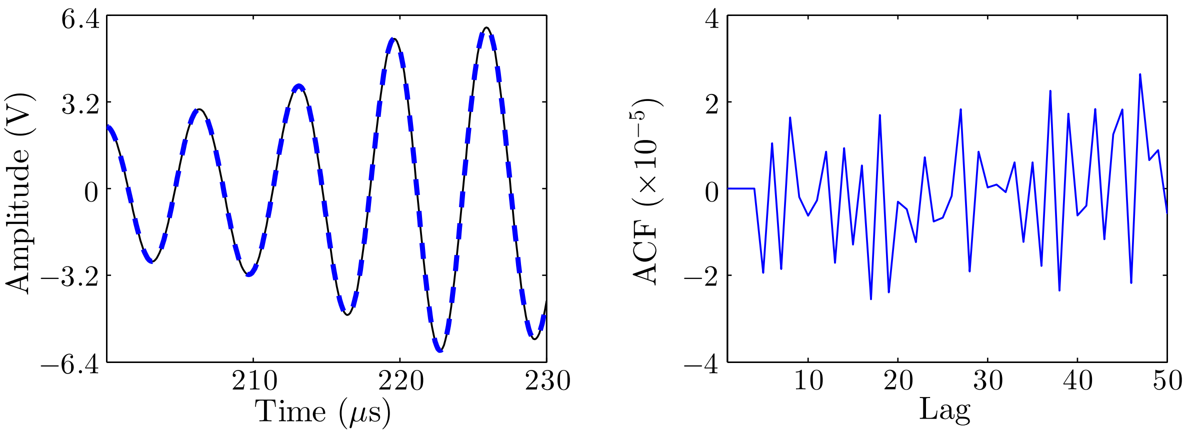

(a) Direct comparison between the certification signal (solid black line ——) and the adjusted signal (dashed blue line – –) with a fit percentage of 99.9.

(b) Residue evaluation of adjusted resposnse.

Source: Created by the author.

Structural prediction is accomplished by the extrapolation of ARX model coefficients

[6]Thereby the next structural identification model series would be obtained/validated with the prediction errors of test numbers 21-30/31-40, respectively, and so on.

for the construction of *theoretical predictive models*. The basic assumption is that the damage evolution follows the same position and type. So, any new damage is inserted in the prediction. Since extrapolation aims to provide the value of a variable out of the range of known values, the trend of the preceding data is taken into account. However, the accuracy expected in the extrapolated coefficients is directly related to their behavior. A visual analysis evidences the complex evolution of coefficient values for the conditions modeled. Thereby, a preliminary approach is to only attempt to predict the response signal of the last damaged condition (0.4 mm of damage depth) taking into account all previous condition tested, as seen in figures 22 and 23. The best extrapolation result was obtained using the spline method[7].

Figure 21 – Mean value and dispersion of standard deviations obtained from prediction errors generated by structural identification models of: ——— reference condition (test numbers 1-20); ——— second damaged condition (0.2 mm of damage depth, test numbers 41-60); ——— fourth damaged condition (0.4 mm of damage depth, test numbers 81-100).

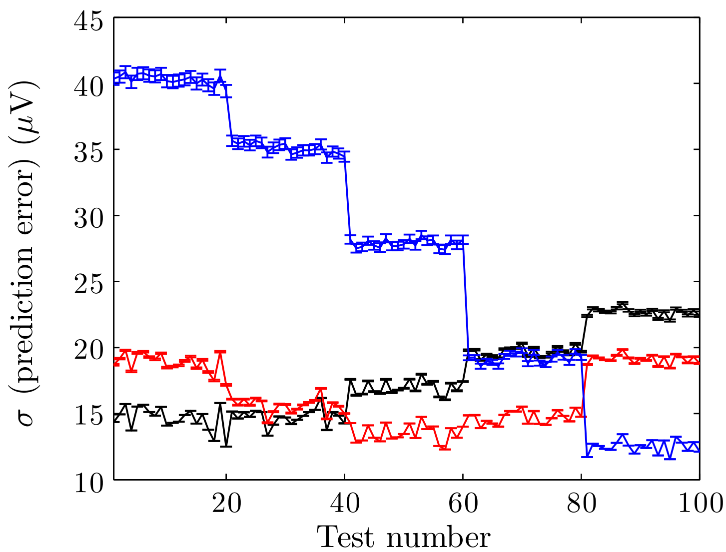

Source: Created by the author.

The computation of these theoretical models follows the opposite way of the autoregressive model estimation presented in APPENDIX B. Thus, the extrapolated coefficients form the polynomials $A(q)$ and $B(q)$ and the predictive response can be estimated. The success of the forecasting procedure is evidenced by figure 24 since the general decreasing behavior of the prediction errors' standard deviation with the increase of damage severity was reproduced. Also, the predictive model generated prediction errors with levels of data dispersion similar to the structural identification models, as well. Therefore, this

[7]Derived from the cubic spline interpolation method.

methodology was able to produce a model to reasonable forecast structural behavior employing only measured data without the need of any physics or mathematical based models.

Figure 22 – Coefficient comparison for polynomial $A(q)$: —— from structural identification models; $*$ – for theoretical predictive model (extrapolated).

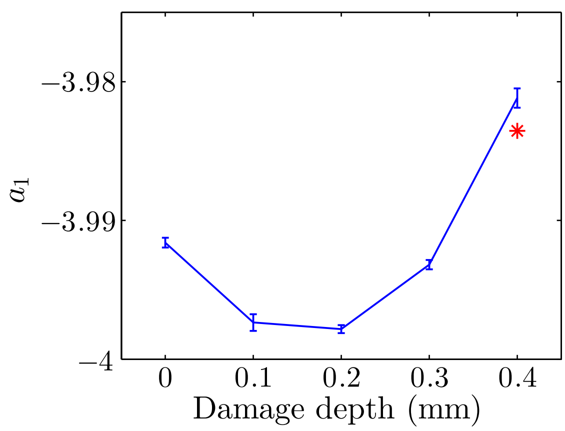

(a) Coefficient a_1.

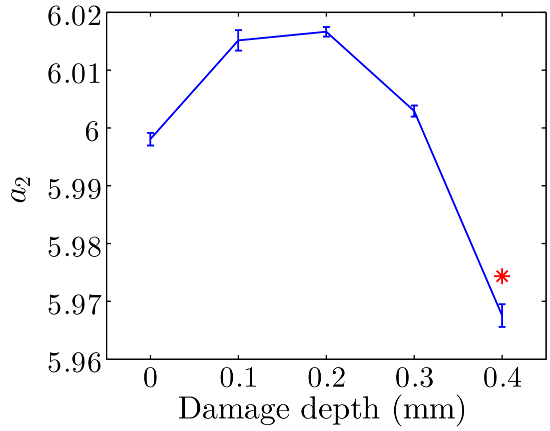

(b) Coefficient a_2.

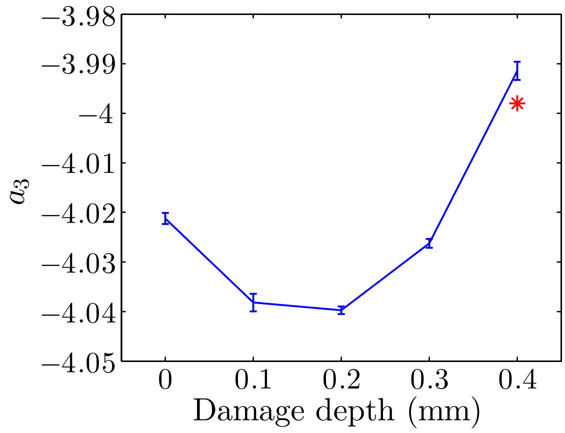

(c) Coefficient a_3.

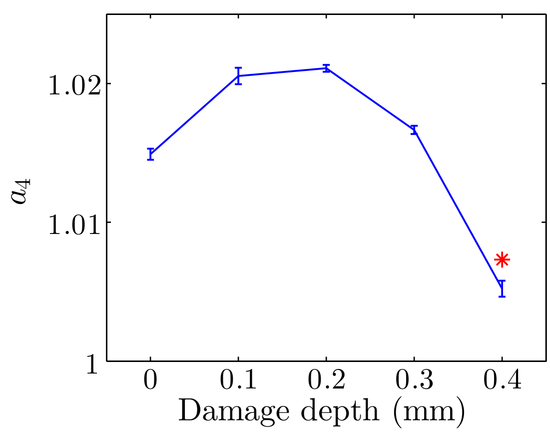

(d) Coefficient a_4.

Source: Created by the author.

Despite of this promising preliminary result in modeling a future damaged condition, it is important to note that only a limited damage scenario was considered. Since wave propagation is ruled by many factors, the right shift of A0 wave packet with damage progression could be interrupted beyond a thickness reduction. This eventual break of pattern could compromise the predictive ability of these theoretical models because of the dependence on coefficient extrapolation. Moreover, damage location and progression remained the same throughout the experiment, what would hardly happen in a real world application. Therefore, the occurrence of a new type of damage or in a different location has to be studied in order to improve prognosis robustness. Finally, the associated inverse problem is not trivial because of the black box nature of ARX models or, in other words, because of their exclusive dependence on the system's response without a clear physical link.

Figure 23 – Coefficient comparison for polynomial $B(q)$: ——— from structural identification models; $*$ – for theoretical predictive model (extrapolated).

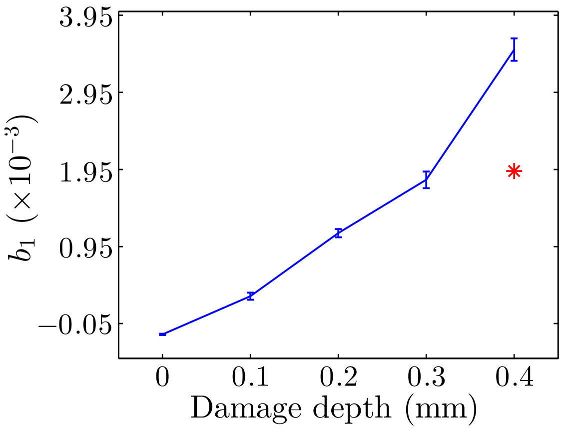

(a) Coefficient b_1.

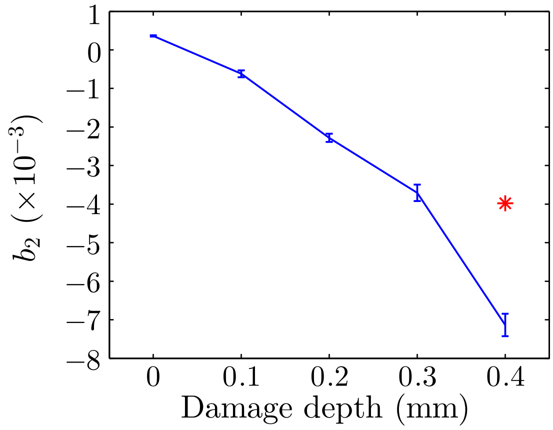

(b) Coefficient b_2.

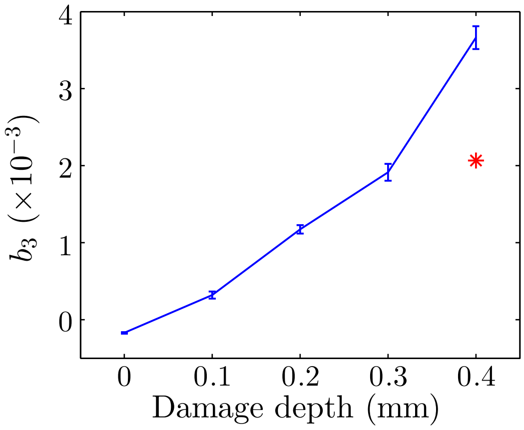

(c) Coefficient b_3.

Source: Created by the author.

4.4 Conclusion

This chapter presented the achievements of a damage detection routine based on statistical process control with the ability to detect discrete levels of a progressive damage as small as 0.1 mm of depth (corresponding to 6.25% in thickness reduction) with statistical confidence. However, it is important to highlight that a high confidence interval of 99.73% had to be used in order to avoid false indications of damage. Also, despite of the caution to keep test conditions constant, some measurement variability was observed throughout the tests which contributed to the increase of the confidence interval as well (temperature variations evidenced by the clear change of damage index value between test numbers 81-90 and 91-100 – last damaged condition). Finally, the statistical distribution of the damage indices could be evaluated to ensure that normal distribution assumption is accepted or the use of other types of data distribution is justified.

Figure 24 – Comparison of the mean value and dispersion of standard deviations obtained from prediction errors generated by the structural identification models for the fourth damaged condition (—— 0.4 mm of damage depth, test numbers 81-100) and the absolute value of this parameter generated by the theoretical predictive model (∗).

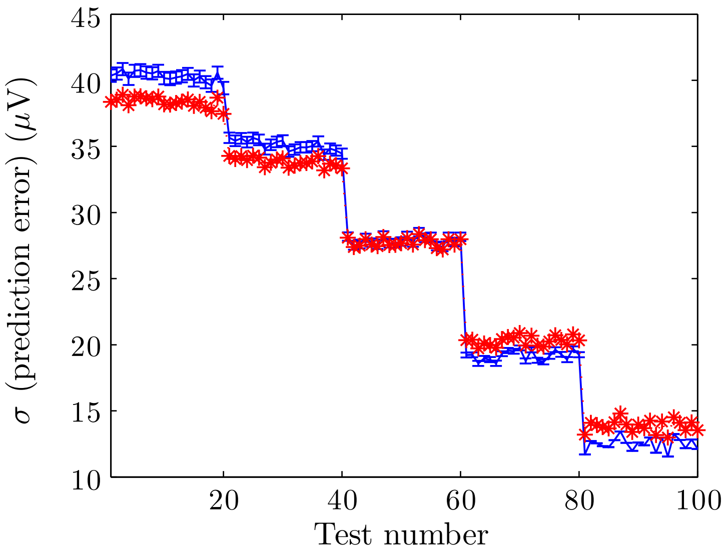

Source: Created by the author.

Moreover, because of the complex behavior of the identified ARX models' coefficients, a preliminary damage prognosis technique was attempted in order to forecast the structure's behavior. This strategy satisfactorily predicted the structure's dynamic response for a damage of 0.4 mm o depth taking into account four previous structural conditions and using the data dispersion verified in the prediction errors as the parameter of evaluation.

The drawbacks of this predictive procedure can be associated with the limited damage scenario considered. To make this methodology more suitable to real world applications, it is desirable to ensure the prognosis of more severe thickness reductions. Also, the occurrence of different types of damage in different locations in a changing environment has to be evaluated. A suggestion to overcome these drawbacks will be to associate an analytical wave propagation model of a plate by spectral elements (SEM) with the coefficients of the ARX model. In this scenario, it would be possible to predict complex damages caused by multiple discontinuities. The idea is to choose a SEM wave model validated with the autoregressive model identified. Future research in this sense is welcome.

5 Final Remarks

In this chapter, the main conclusions achieved in this work are discussed. Also, suggestions for future research are presented.

5.1 Conclusion

This work studied the influence of operational and environmental conditions on damage detection with the creation of a monitoring method capable of separating the effects of loading from those of damage. It was evidenced that this topic is a crucial issue to become SHM suitable for real world applications. Additionally, damage prognosis was investigated and a primary technique was developed. In this sense, the main conclusions provided by the review of relevant works presented in chapter 2 are listed below:

- A feasible strategy to perform SHM is to develop techniques based only on time signal processing together with statistical models;
- Compensation procedures are suitable in order to separate the effects of undesirable factors, such as temperature and load, from the effects of damage in an early stage of a monitoring technique;
- Unsupervised learning algorithms are preferred since only data from the undamaged structure for their training. Also, their automatic nature and relatively simple development makes them attractive for on-board wireless applications;
- Damage prognosis is a natural evolution of SHM because of its capacity to optimize the useful life of a structure;
- To do so, it is fundamental to have a predictive model to track the changes associated to damage evolution.

Thus, both techniques presented in this work followed the time series processing paradigm employing Lamb waves for structural interrogation and system modeling by autoregressive models. Such models are useful to provide a parametrization of the structure's reference condition and to generate prediction errors which are sensitive to structural changes. Also, they enable the creation of prognosis models, eschewing the need of intricate physics or mathematical based models, through the extrapolation of coefficients in a attempt to forecast the future behavior of a damaged structure. Besides, the use of autoregressive models is justified by their simple implementation and certification. In this sense, some conclusions can be highlighted from both experiments:

- A novel procedure of modeling the reference Lamb signal by an AR model was performed in a way so the prediction errors carried information about load changes and damage evolution as well;
- The signal feature extraction was performed on the prediction errors to feed the fuzzy c-means classification for effect separation;
- The classification of effects that acted on the structure throughout the experiment was successful mainly because of the knowledge of such conditions;
- This analysis of input effects could be an issue for real world cases because all the sources of measurement variability are not always known;
- A similar procedure was carried for the prognosis strategy with a two step model identification resulting in a successful detection of all damage tested with statistical confidence using statistical process control;
- The damage prognosis methodology was performed by coefficient extrapolation to create a parametrization of the structure's response for a damage depth of 0.4 mm without the need of any complex white box models;
- The procedure performance was only evaluated for a limited level of damage and varying conditions.

These topics lead to suggestions to be tested in future works in order to improve damage prognosis in structures subjected to operational and environmental conditions which are discussed in the next section.

5.2 Suggestions for Future Research

In this section some suggestions for further research are provided based on what was verified in the experiments developed in this work:

- Although the separation of effects performed in chapter 3 showed satisfactory results, a more realistic procedure for real world monitoring online must rely on methods that are able to distinguish the distinct effects that the structure is subjected continuously;

- A compensation procedure could be easily associated to the signal processing of the predictive technique developed in chapter 4 to eliminate the effects of varying conditions (such as temperature) resulting in a reliable damage prognosis even under the influence of operational and environmental variability;

- Damage prognosis robustness could be tested for more severe damage since the propagation pattern might change in such case;

- To overcome these drawbacks, a spectral element model (SEM) could be identified and the physical parameters and boundary conditions associated with damages. This SEM could be used for tracking AR model coefficients to procedure the prediction based on time series analysis using the experimental data.

References

ALBAKRI, M.; TARAZAGA, P. Spectral element based optimization scheme for damage identification. In: **Structural Health Monitoring, Volume 5**. Springer, 2014. p. 19–27. Available at: <http://dx.doi.org/10.1007/978-3-319-04570-2_3>. Access on: 22 June 2015.

ALLEYNE, D. N.; CAWLEY, P. The interaction of lamb waves with defects. **Ultrasonics, Ferroelectrics, and Frequency Control, IEEE Transactions on**, IEEE, v. 39, n. 3, p. 381–397, 1992. Available at: <http://dx.doi.org/10.1109/58.143172>. Access on: 22 June 2015.

______. Optimization of lamb wave inspection techniques. **Ndt & E International**, Elsevier, v. 25, n. 1, p. 11–22, 1992. Available at: <http://dx.doi.org/10.1016/0963-8695(92)90003-Y>. Access on: 22 June 2015.

BAPTISTA, F. G.; FILHO, J. V. A new impedance measurement system for pzt-based structural health monitoring. **Instrumentation and Measurement, IEEE Transactions on**, IEEE, v. 58, n. 10, p. 3602–3608, 2009. Available at: <http://dx.doi.org/10.1109/TIM.2009.2018693>. Access on: 22 June 2015.

BAPTISTA, F. G.; FILHO, J. V.; INMAN, D. J. Real-time multi-sensors measurement system with temperature effects compensation for impedance-based structural health monitoring. **Structural Health Monitoring**, SAGE Publications, v. 11, n. 2, p. 173–186, 2012. Available at: <http://dx.doi.org/10.1177/1475921711414234>. Access on: 22 June 2015.

BEZDEK, J. C. **Pattern recognition with fuzzy objective function algorithms**. [S.l.]: Kluwer Academic Publishers, 1981.

BEZDEK, J. C.; PAL, S. K. **Fuzzy models for pattern recognition**. [S.l.]: IEEE press New York, 1992.

BHALLA, S.; NAIDU, A. S.; SOH, C. K. Influence of structure-actuator interactions and temperature on piezoelectric mechatronic signatures for nde. In: INTERNATIONAL SOCIETY FOR OPTICS AND PHOTONICS. **Smart Materials, Structures, and Systems**. 2003. p. 263–269. Available at: <http://dx.doi.org/10.1117/12.514762>. Access on: 22 June 2015.

BOX, G.; JENKINS, G.; REINSEL, G. **Time Series Analysis: Forecasting and Control**. New Jersey: Pretince Hall, 1994.

CAWLEY, P.; ALLEYNE, D. The use of lamb waves for the long range inspection of large structures. **Ultrasonics**, Elsevier, v. 34, n. 2, p. 287–290, 1996. Available at: <http://dx.doi.org/10.1016/0041-624X(96)00024-8>. Access on: 22 June 2015.

CHANG, P. C.; FLATAU, A.; LIU, S. Review paper: health monitoring of civil infrastructure. **Structural health monitoring**, Sage Publications, v. 2, n. 3, p. 257–267, 2003. Available at: <http://dx.doi.org/10.1177/1475921703036169>. Access on: 22 June 2015.

CHATTOPADHYAY, A. et al. **A Multidisciplinary Approach to Health Monitoring and Materials Damage Prognosis for Metallic Aerospace Systems**. [S.l.], 2013. Available at: <http://www.dtic.mil/cgi-bin/GetTRDoc?Location=U2doc=GetTRDoc-.pdfAD=ADA587226>. Access on: 22 June 2015.

CROSS, E. J.; WORDEN, K.; CHEN, Q. Cointegration: a novel approach for the removal of environmental trends in structural health monitoring data. **Proceedings of the Royal Society A: Mathematical, Physical and Engineering Science**, v. 467, n. 2133, p. 2712–2732, 2011. Available at: <http://rspa.royalsocietypublishing.org/content-/467/2133/2712.abstract>. Access on: 22 June 2015.

CROXFORD, A. J. et al. Efficient temperature compensation strategies for guided wave structural health monitoring. **Ultrasonics**, Elsevier, v. 50, n. 4, p. 517–528, 2010. Available at: <http://dx.doi.org/10.1016/j.ultras.2009.11.002>. Access on: 22 June 2015.

______. Quantification of environmental compensation strategies for guided wave structural health monitoring. In: INTERNATIONAL SOCIETY FOR OPTICS AND PHOTONICS. **The 15th International Symposium on: Smart Structures and Materials & Nondestructive Evaluation and Health Monitoring**. 2008. p. 69350H–69350H. Available at: <http://dx.doi.org/10.1117/12.776362>. Access on: 22 June 2015.

DALTON, R.; CAWLEY, P.; LOWE, M. The potential of guided waves for monitoring large areas of metallic aircraft fuselage structure. **Journal of Nondestructive Evaluation**, Springer, v. 20, n. 1, p. 29–46, 2001. Available at: <http://dx.doi.org/10-.1023/A:1010601829968>. Access on: 22 June 2015.

DOEBLING, S. W. et al. A summary review of vibration-based damage identification methods. **Shock and vibration digest**, Citeseer, v. 30, n. 2, p. 91–105, 1998. Available at: <http://citeseerx.ist.psu.edu/viewdoc/download?doi=10.1.1.57.9721rep=rep1type=pdf>. Access on: 22 June 2015.

FARRAR, C. R. **Damage prognosis: current status and future needs**. Los Alamos, NM, 2003. Access on: 22 June 2014.

FARRAR, C. R.; LIEVEN, N. A. Damage prognosis: the future of structural health monitoring. **Philosophical Transactions of the Royal Society A: Mathematical, Physical and Engineering Sciences**, The Royal Society, v. 365, n. 1851, p. 623–632, 2007. Available at: <http://dx.doi.org/10.1098/rsta.2006.1927>. Access on: 22 June 2015.

FARRAR, C. R.; SOHN, H. Pattern recognition for structural health monitoring. In: **Workshop on Mitigation of Earthquake Disaster by Advanced Technologies**. [s.n.], 2000. Available at: <http://institute.lanl.gov/ei/shm/pubs/mceer_00.pdf>. Access on: 22 June 2015.

FARRAR, C. R.; WORDEN, K. An introduction to structural health monitoring. **Philosophical Transactions of the Royal Society A: Mathematical, Physical

and Engineering Sciences, The Royal Society, v. 365, n. 1851, p. 303–315, 2007. Available at: <http://dx.doi.org/10.1098/rsta.2006.1928>. Access on: 22 June 2015.

FASSOIS, S. D.; SAKELLARIOU, J. S. Time-series methods for fault detection and identification in vibrating structures. **Philosophical Transactions of the Royal Society A: Mathematical, Physical and Engineering Sciences**, The Royal Society, v. 365, n. 1851, p. 411–448, 2007. Available at: <http://dx.doi.org/10.1098/rsta.2006.1929>. Access on: 22 June 2015.

FIGUEIREDO, E. et al. Machine learning algorithms for damage detection under operational and environmental variability. **Structural Health Monitoring**, SAGE Publications, v. 10, n. 6, p. 559–572, 2011. Available at: <http://dx.doi.org/10.1177-/1475921710388971>. Access on: 22 June 2015.

_____. **Structural health monitoring algorithm comparisons using standard data sets**. [S.l.], 2009. Available at: <http://dx.doi.org/10.2172/961604>. Access on: 22 June 2015.

_____. Autoregressive modeling with state-space embedding vectors for damage detection under operational variability. **International Journal of Engineering Science**, Elsevier, v. 48, n. 10, p. 822–834, 2010. Available at: <http://dx.doi.org/10.1016/j.ijengsci-.2010.05.005>. Access on: 22 June 2015.

FRITZEN, C.-P.; KRAEMER, P. Self-diagnosis of smart structures based on dynamical properties. **Mechanical Systems and Signal Processing**, Elsevier, v. 23, n. 6, p. 1830–1845, 2009. Available at: <http://dx.doi.org/10.1016/j.ymssp.2009.01.006>. Access on: 22 June 2015.

FUGATE, M. L.; SOHN, H.; FARRAR, C. R. Unsupervised learning methods for vibration-based damage detection. In: **Proceedings of 18th International Modal Analysis Conference–IMAC**. [s.n.], 2000. p. 18. Available at: <http://citeseerx.ist-.psu.edu/viewdoc/download?doi=10.1.1.4.3039rep=rep1type=pdf>. Access on: 22 June 2015.

GIURGIUTIU, V. Current issues in vibration-based fault diagnostics and prognostics. In: INTERNATIONAL SOCIETY FOR OPTICS AND PHOTONICS. **NDE For Health Monitoring and Diagnostics**. 2002. p. 101–112. Available at: <http://dx.doi.org/10.1117/12.469869>. Access on: 22 June 2015.

HU, N. et al. Identification of delamination position in cross-ply laminated composite beams using s 0 lamb mode. **Composites Science and Technology**, Elsevier, v. 68, n. 6, p. 1548–1554, 2008.

INMAN, D. Smart structures: examples and new problems. In: **Proceedings of 16th Brazilian Congress of Mechanical Engineering–COBEM 2001**. [S.l.: s.n.], 2001.

INMAN, D. J. et al. **Damage prognosis**. Chichester, UK: John Wiley & Sons, Ltd, 2005. Available at: <http://dx.doi.org/10.1002/0470869097.fmatter>. Access on: 22 June 2015.

KULKARNI, S.; ACHENBACH, J. Structural health monitoring and damage prognosis in fatigue. **Structural Health Monitoring**, SAGE Publications, v. 7, n. 1, p. 37–49, 2008. Available at: <http://dx.doi.org/10.1177/1475921707081973>. Access on: 22 June 2015.

LEE, B.; STASZEWSKI, W. Modelling of lamb waves for damage detection in metallic structures: Part ii. wave interactions with damage. **Smart Materials and Structures**, IOP Publishing, v. 12, n. 5, p. 815, 2003. Available at: <http://dx.doi.org/10.1088/0964-1726/12/5/019>. Access on: 22 June 2015.

LEMISTRE, M.; BALAGEAS, D. Structural health monitoring system based on diffracted lamb wave analysis by multiresolution processing. **Smart materials and structures**, IOP Publishing, v. 10, n. 3, p. 504, 2001.

LIM, H. J. et al. Impedance based damage detection under varying temperature and loading conditions. **NDT & E International**, Elsevier, v. 44, n. 8, p. 740–750, 2011. Available at: <http://dx.doi.org/10.1016/j.ndteint.2011.08.003>. Access on: 22 June 2015.

LING, Y.; MAHADEVAN, S. Integration of structural health monitoring and fatigue damage prognosis. **Mechanical Systems and Signal Processing**, Elsevier, v. 28, p. 89–104, 2012. Available at: <http://dx.doi.org/10.1016/j.ymssp.2011.10.001>. Access on: 22 June 2015.

LJUNG, L. **System identification**. 2. ed. Upper Saddle River, NJ: Prentice-Hall PTR, 1998.

LOPES Jr, V.; CHANG, F.-K. Damage identification in composite structures using artificial neural network. In: BCCM. **1st Brazilian Conference on Composite Materials**. Natal, RN, Brazil, 2012. p. 1–6.

LOPES Jr, V. et al. Characterization of the temperature, load and damage effects using piezoelectric transducer patches based on fuzzy clustering. In: IWSHM. **8th International Workshop on Structural Health Monitoring 2011**. Stanford, California, USA, 2011. p. 1196–1205.

LU, Y.; GAO, F. A novel time-domain auto-regressive model for structural damage diagnosis. **Journal of Sound and Vibration**, Elsevier, v. 283, n. 3, p. 1031–1049, 2005. Available at: <http://dx.doi.org/10.1016/j.jsv.2004.06.030>. Access on: 22 June 2015.

LU, Y.; MICHAELS, J. E. A methodology for structural health monitoring with diffuse ultrasonic waves in the presence of temperature variations. **Ultrasonics**, Elsevier, v. 43, n. 9, p. 717–731, 2005. Available at: <http://dx.doi.org/10.1016/j.ultras.2005.05.001>. Access on: 22 June 2015.

MONTGOMERY, D. C. **Introduction to statistical quality control**. 3. ed. [S.l.]: John Wiley & Sons, Inc, 1996.

PARK, G.; CUDNEY, H. H.; INMAN, D. J. Impedance-based health monitoring of civil structural components. **Journal of infrastructure systems**, American Society of Civil Engineers, v. 6, n. 4, p. 153–160, 2000. Available at: <http://dx.doi.org/10.1061-/(ASCE)1076-0342(2000)6:4(153)>. Access on: 22 June 2015.

PARK, G. et al. Impedance-based structural health monitoring for temperature varying applications. **JSME international journal. Series A, Solid mechanics and material engineering**, Japan Society of Mechanical Engineers, v. 42, n. 2, p. 249–258, 1999. Available at: <http://ci.nii.ac.jp/naid/110002965363/>. Access on: 22 June 2015.

_____. Overview of piezoelectric impedance-based health monitoring and path forward. **Shock and Vibration Digest**, Washington, DC: The Center, v. 35, n. 6, p. 451–464, 2003. Available at: <http://cat.inist.fr/?aModele=afficheNcpsidt=15280692>. Access on: 22 June 2015.

PARK, S. et al. Electro-mechanical impedance-based wireless structural health monitoring using pca-data compression and k-means clustering algorithms. **Journal of Intelligent Material Systems and Structures**, Sage Publications, v. 19, n. 4, p. 509–520, 2008. Available at: <http://dx.doi.org/10.1177/1045389X07077400>. Access on: 22 June 2015.

PAVLOPOULOU, S.; WORDEN, K.; SOUTIS, C. Structural health monitoring and damage prognosis in composite repaired structures through the excitation of guided ultrasonic waves. In: INTERNATIONAL SOCIETY FOR OPTICS AND PHOTONICS. **SPIE Smart Structures and Materials+ Nondestructive Evaluation and Health Monitoring**. 2013. p. 869504–869504. Available at: <http://dx.doi.org/10.1117/12.2009346>. Access on: 22 June 2015.

RAGHAVAN, A.; CESNIK, C. E. Review of guided-wave structural health monitoring. **Shock and Vibration Digest**, Washington, DC: The Center, v. 39, n. 2, p. 91–116, 2007. Available at: <http://dx.doi.org/10.1177/0583102406075428>. Access on: 22 June 2015.

RYTTER, A.; KIRKEGAARD, P. H. **Vibration based inspection of civil engineering structures**. [S.l.]: Aalborg Universitetsforlag, 1994.

SILVA, S.; DIAS Jr, M.; LOPES Jr, V. Damage detection in a benchmark structure using ar-arx models and statistical pattern recognition. **Journal of the Brazilian Society of Mechanical Sciences and Engineering**, SciELO Brasil, v. 29, n. 2, p. 174–184, 2007. Available at: <http://dx.doi.org/10.1590/S1678-58782007000200007>. Access on: 22 June 2015.

_____. Structural health monitoring in smart structures through time series analysis. **Structural Health Monitoring**, SAGE Publications, v. 7, n. 3, p. 231–244, 2008. Available at: <http://dx.doi.org/10.1177/1475921708090561>. Access on: 22 June 2015.

SILVA, S. et al. Structural damage detection by fuzzy clustering. **Mechanical Systems and Signal Processing**, Elsevier, v. 22, n. 7, p. 1636–1649, 2008. Available at: <http://dx.doi.org/10.1016/j.ymssp.2008.01.004>. Access on: 22 June 2015.

SILVA, S.; GONSALEZ, C. G.; LOPES Jr, V. Adaptive filter feature identification for structural health monitoring in an aeronautical panel. **Structural Health Monitoring**, SAGE Publications, v. 10, n. 5, p. 481–489, 2011. Available at: <http://dx.doi.org/10.1177/1475921710379514>. Access on: 22 June 2015.

SOHN, H. Effects of environmental and operational variability on structural health monitoring. **Philosophical Transactions of the Royal Society A: Mathematical, Physical and Engineering Sciences**, The Royal Society, v. 365, n. 1851, p. 539–560, 2007. Available at: <http://dx.doi.org/10.1098/rsta.2006.1935>. Access on: 22 June 2015.

SOHN, H.; CZARNECKI, J. A.; FARRAR, C. R. Structural health monitoring using statistical process control. **Journal of Structural Engineering**, American

Society of Civil Engineers, v. 126, n. 11, p. 1356–1363, 2000. Available at: <http://dx.doi.org/10.1061/(ASCE)0733-9445(2000)126:11(1356)>. Access on: 22 June 2015.

SOHN, H. et al. An experimental study of temperature effect on modal parameters of the alamosa canyon bridge. **Earthquake engineering & structural dynamics**, v. 28, n. 8, p. 879–897, 1999. Available at: <http://dx.doi.org/10.1002/(SICI)1096-9845(199908)28:8<879::AID-EQE845>3.0.CO;2-V>. Access on: 22 June 2015.

SOHN, H.; FARRAR, C. R. Damage diagnosis using time series analysis of vibration signals. **Smart materials and structures**, IOP Publishing, v. 10, n. 3, p. 446, 2001. Available at: <http://dx.doi.org/10.1088/0964-1726/10/3/304>. Access on: 22 June 2015.

SOHN, H. et al. Structural health monitoring using statistical pattern recognition techniques. **Transactions-American Society of Mechanical Engineers Journal of Dynamic Systems Measurement And Control**, Citeseer, v. 123, n. 4, p. 706–711, 2001. Available at: <http://institutes.lanl.gov/ei/shm/pubs/jdsmc_01.pdf>. Access on: 22 June 2015.

SOHN, H.; WORDEN, K.; FARRAR, C. R. Statistical damage classification under changing environmental and operational conditions. **Journal of Intelligent Material Systems and Structures**, Sage Publications, v. 13, n. 9, p. 561–574, 2002. Available at: <http://dx.doi.org/10.1106/104538902030904>. Access on: 22 June 2015.

SU, Z.; YE, L. **Identification of damage using Lamb waves: from fundamentals to applications**. Springer Science & Business Media, 2009. Available at: <http://dx.doi.org/10.1007/978-1-84882-784-4>. Access on: 22 June 2015.

SUN, F. P. et al. Automated real-time structure health monitoring via signature pattern recognition. **Proc. SPIE Smart Structures and Materials 1995: Smart Structures and Integrated Systems**, v. 2443, 1995. Available at: <http://dx.doi.org/10.1117/12.208261>. Access on: 22 June 2015.

TAN, K. et al. Experimental evaluation of delaminations in composite plates by the use of lamb waves. **Composites science and technology**, Elsevier, v. 53, n. 1, p. 77–84, 1995.

TOYAMA, N.; TAKATSUBO, J. Lamb wave method for quick inspection of impact-induced delamination in composite laminates. **Composites science and technology**, Elsevier, v. 64, n. 9, p. 1293–1300, 2004.

WILCOX, P. et al. A comparison of temperature compensation methods for guided wave structural health monitoring. In: **AIP Conference Proceedings**. [s.n.], 2008. v. 975, p. 1453. Available at: <http://dx.doi.org/10.1063/1.2902606>. Access on: 22 June 2015.

WILCOX, P.; LOWE, M.; CAWLEY, P. Mode and transducer selection for long range lamb wave inspection. **Journal of intelligent material systems and structures**, SAGE Publications, v. 12, n. 8, p. 553–565, 2001. Available at: <http://dx.doi.org/10.1177/10453890122145348>. Access on: 22 June 2015.

WORDEN, K.; DULIEU-BARTON, J. An overview of intelligent fault detection in systems and structures. **Structural Health Monitoring**, SAGE Publications, v. 3, n. 1, p. 85–98, 2004. Available at: <http://dx.doi.org/10.1177/1475921704041866>. Access on: 22 June 2015.

WORDEN, K. et al. The fundamental axioms of structural health monitoring. **Proceedings of the Royal Society A: Mathematical, Physical and Engineering Science**, The Royal Society, v. 463, n. 2082, p. 1639–1664, 2007. Available at: <http://dx.doi.org/10.1098/rspa.2007.1834>. Access on: 22 June 2015.

WORDEN, K.; MANSON, G.; FIELLER, N. Damage detection using outlier analysis. **Journal of Sound and Vibration**, Elsevier, v. 229, n. 3, p. 647–667, 2000. Available at: <http://dx.doi.org/10.1006/jsvi.1999.2514>. Access on: 22 June 2015.

APPENDIX A – Lamb Waves

Lamb waves is a class of guided waves which occur in thin plates whose movement happens in the plan that contains the propagation direction and in the normal plan resulting in a superposition of longitudinal and shear modes. This kind of wave was discovery by Horace Lamb in 1917 presenting the following expressions for symmetric or antisymmetric mode, respectively[1] (RAGHAVAN; CESNIK, 2007):

$$\frac{\tan(\beta h)}{\tan(\alpha h)} = -\frac{4\alpha\beta\xi^2}{(\xi^2 - \beta^2)^2} \tag{10}$$

$$\frac{\tan(\beta h)}{\tan(\alpha h)} = -\frac{(\xi^2 - \beta^2)^2}{4\alpha\beta\xi^2} \tag{11}$$

in which the terms α, β and ξ are defined as:

$$\alpha^2 = \frac{\omega^2}{c_L^2} - \xi^2, \qquad \beta^2 = \frac{\omega^2}{c_T^2} - \xi^2, \qquad \xi = \frac{\omega}{c_p}$$

where h is the plate thickness, ξ is the wavenumber, c_L and c_T are the velocities of longitudinal and transverse modes, c_p is the phase velocity and ω is the wave circular frequency.

Lamb waves present great propagation capacity and high susceptibility to interference on a propagation path making them suitable for structural inspection since the diagnosis is based on the comparison of sent and received signals. Besides, Lamb waves produce mechanical stress through the whole plate thickness leading to structural interrogation capable of detecting surface or internal damage (ALLEYNE; CAWLEY, 1992b).

To do so, a good inspection requires the choice of a input signal with a single mode because the presence of multiple modes in the response signal can be used as a damage indicator (CAWLEY; ALLEYNE, 1996). The basic factors that determine which mode and frequency must be used are (WILCOX et al., 2001): (a) dispersion; (b) attenuation; (c) sensitivity; (d) excitability; (e) detectability; (f) selectivity.

[1] See Su and Ye (2009) for a complete development of the equations that rule the motion of Lamb waves.

Figure 25 – Lamb wave modes.

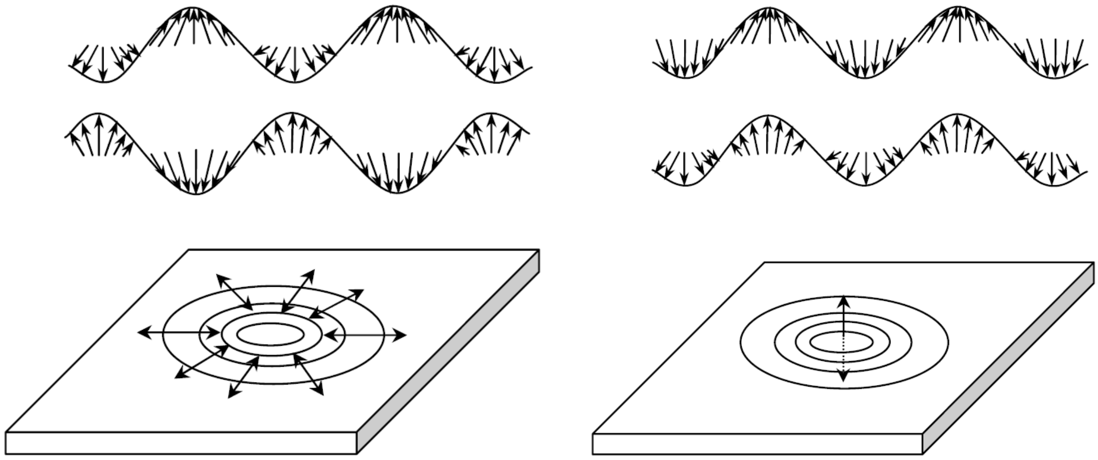

(a) Radial in-plane motion caused by the symmetric mode.

(b) Out-of-plane motion caused by the antisymmetric mode.

Source: Su and Ye (2009) – adapted.

Equation (11) correlates the propagation velocity with the frequency indicating that this kind of wave, regardless of mode, is dispersive. In other words, propagation velocity is dependent of frequency. Since dispersion will cause changes in the shape of the wave packet, it can affect damage detection[2] (ALLEYNE; CAWLEY, 1992b). As an example, Wilcox et al. (2001) tested different modes with many frequency based on these factors concluding that narrow frequency band signals better prevent wave dispersion justifying the common choice of windowed pure tones to ensure a successful monitoring (see figures 3(c) and 13(a)).

Another important factor is the inspection distance, specially in one-dimensional structures such as pipes and rails, which is limited by material attenuation. This adversity can be mitigated by the increase of input power achieved with the use of amplifiers and selection of enhanced sensors. Also, a crucial issue is to ensure damage sensitivity to the excitation wave. A common practice is to set the wavelength to be at least half of the expected damage size since the sensitivity generally increases as the wavelength decreases (DALTON et al., 2001; ALLEYNE; CAWLEY, 1992a). However, it is known that different damage geometries are sensitive to specific wave characteristics such as frequency-thickness product, mode type (symmetric or antisymmetric) and mode order (ALLEYNE; CAWLEY, 1992a). This was verified in the present work as for the composite structure the packet S0 was found to be more sensitive to delamination while for the aluminum plate the A0

[2]The correlation of propagation speed and frequency is evidenced by the phase velocity graph presented in figures 3(c) and 13(c). It is important to note that the dispersion can be avoided by the adequate actuation frequency selection. For example, lower frequencies will generate a non-dispersive first symmetric package (S0) since its phase velocity is almost flat in this region.

packet was chosen to monitor local mass loss.

So far, factors (a)-(c) dealt exclusively with the monitored system. On the other hand, factors (d)-(f) are related to the requirements that the transducer scheme will have to achieve in order to produce the chosen wave frequency and mode and to measure the vibration response. A detailed procedure for this evaluation can be found in Wilcox et al. (2001), Su and Ye (2009).

APPENDIX B – Autoregressive Models

A process or system's behavior can be identified by autoregressive models providing a time domain parametric representation. Such models are obtained through the measurement of vibratory signals imposed to a structure deriving from a general expression (LJUNG, 1998):

$$A(q)y(k) = \frac{B(q)}{F(q)}u(k) + \frac{C(q)}{D(q)}e(k) \tag{12}$$

where $A(q)$, $B(q)$, $C(q)$, $D(q)$ and $F(q)$ are polynomials that act on the input and output signal – $u(k)$ and $y(k)$, respectively – and on the prediction error $e(k)$ which corresponds to the portion of the output signal that the identification process is not able to reproduce and must be strictly random. The simplification $B(q) = C(q) = D(q) = F(q) = 1$ on equation (12) results in the AR model (outlined in figure 26):

$$A(q)y(k) = e(k) \tag{13}$$

Figure 26 – Schematic representation of the AR model.

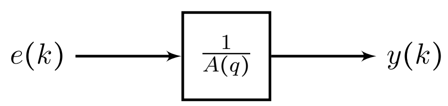

Source: Created by the author.

This implies that the prediction error only depends on the output signal multiplied by $A(q)$ which can be estimated by many methods, such as the ordinary least squares procedures or the Yule-Walker equations (BOX et al., 1994). On the other hand, this polynomial is dependent of the backshift operator[1] and is described as follows:

$$A(q) = 1 - a_1 q^{-1}, \cdots, a_{n_a} q^{n_a} \tag{14}$$

where a_i are model's parameters for $i = 1, 2, \cdots, n_a$ and n_a is the regression order of the

[1]For example: $y(k)q^{-1} = y(k-1)$.

model's polynomial. Thus, it is possible to define the system's response as a function of the other parameters for a reference condition:

$$y_{ref}(k) = \sum_{i=1}^{n_a} a_i y_{ref}(k-i) + e_{y_{ref}}(k) \tag{15}$$

and for an unknown condition as well:

$$y_{unk}(k) = \sum_{i=1}^{n_a} a_i y_{unk}(k-i) + e_{y_{unk}}(k) \tag{16}$$

Reference models (for health condition) are associated to prediction errors $e_{y_{ref}(k)}$ that are only obtained for data with that same specific condition. These terms can also be defined for both reference and unknown condition:

$$e_{y_{ref}}(k) = y_{ref}(k) + \hat{y}_{ref}(k) \tag{17}$$

$$e_{y_{unk}}(k) = y_{unk}(k) + \hat{y}_{unk}(k) \tag{18}$$

where $y_{ref}(k)$ and $y_{unk}(k)$ are certification signals and $\hat{y}_{ref}(k)$ and $\hat{y}_{unk}(k)$ are signals adjusted by the model. Prediction errors can be statistically analyzed providing a reliable way to evaluate changes in a monitored system. Once significant changes in the prediction errors are observed a reference model is unable to reproduce this new operating status indicating system's dynamic alterations (SILVA et al., 2007).

Order Determination

A primordial issue for the creation of autoregressive models is related to polynomial order determination because this information is unknown a priori. One way to determine the order or number of parameters of a linear system is to use some specific criteria. The two most used methods are the final prediction error (FPE) and the Akaike's information criterion (AIC). The latter method is the one employed in this work, which is defined as (LJUNG, 1998):

$$AIC(n_\theta) = N \ln[\sigma^2_{error}(n_\theta)] + 2n_\theta \tag{19}$$

where N is the number of samples, $\sigma^2_{error}(n_\theta)$ is prediction error's variance and n_θ is the total number of estimated coefficients.

This criterion computes the addition of a new term and its contribution in decreasing the term $\sigma^2_{error}(n_\theta)$. Thus, the increase in the number of coefficients leads to a prediction error decrease resulting in a better data adjustment. However, as the number of coefficients increases, the minimization effect in the prediction error becomes insignificant getting to a point in which the addition of a new term is not justified. Therefore the first term of equation (19) quantifies the prediction error's variance reduction while the second term penalizes the addition of a new term. Thereby, AIC index minimization leads to a well adjusted model due to the prediction error's low variance with a sufficiently low number of terms.

Model Validation

A good system identification is guaranteed with proper model validation since model orders can be determined by the AIC index minimization, which generates a range of candidate orders. This fact implies that a verification must be performed in order to ensure the model's success in reproducing the system's behavior. It is important to note that this procedure requires different data from those used to create the model.

This step is performed in the present work by the direct comparison between the estimated and the validation signal with the adjustment percentage or, in other words, the amount of the real signal reproduced by the model:

$$fit = 100\left\{1 - \frac{||\hat{y}(k) - y(k)||}{||y(k) - \mu[y(k)]||}\right\} \tag{20}$$

where $y(k)$ is the signal for validation, $\hat{y}(k)$ is the adjusted signal and $\mu(*)$ is mean operator. Also, the autocorrelation function (ACF) is calculated to evaluate the prediction error's random behavior which should result in virtually null residue correlation with past samples inside a confidence interval (LJUNG, 1998).

APPENDIX C – Time-Frequency Analysis – Trace Index

As mentioned in chapter 3, the trace index calculation is carried through time-frequency domain decomposition associated to singular value decomposition in order to extract structural information. The overview of this procedure is outlined in figure 27.

Figure 27 – Overview of the trace index calculation.

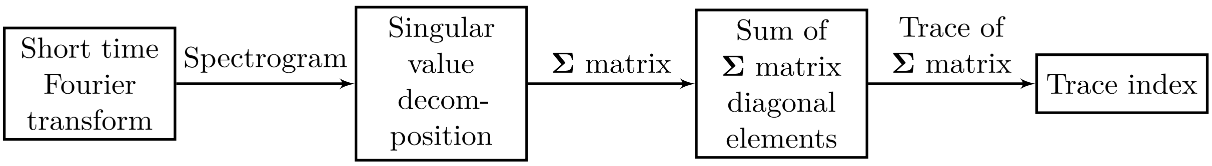

Source: Created by the author.

Time-frequency analysis refers to the techniques capable to investigate signals in both time and frequency domain. This processing tools is useful to investigate signals whose behavior change in time or, in other words, are transient. Lamb waves are a good example of transient signals as seen in figures 3(b), 13(b). Among many methods available for this end, the short-time Fourier transform (STFT) extracts frequency and phase information from sections of a time signal. The discrete STFT is computed by multiplying parts of the prediction error $e(k)$ by a window function $w(k)$ in the following way:

$$STFT[e(k)](l,f) = E(l,f) = \sum_{l=-\infty}^{\infty} e(k)w(k-l)\mathbf{e}^{-2\pi \mathbf{j} ft} \tag{21}$$

where $\mathbf{e}$ is the Naperian base, $\mathbf{j}$ is the imaginary number, l and f are the resulting time and frequency discrete samples, respectively. Usually the term $w(k)$ is a Hann window whose shape resemble the envelope of the Gaussian tone-burst (figures 3(a), 13(a)). Some amount of overlap between the windowed signal blocks is used to reduce discontinuities. In practical applications the STFT is computed by the Fast Fourier Transform algorithm. For the present application best results were obtained for a signal length of 128 points with 50% of overlap whose frequency decomposition interval ranged from 50 kHz to 500 kHz as seen in figure 28.

Figure 28 – Power spectral density of the time-frequency decomposition.

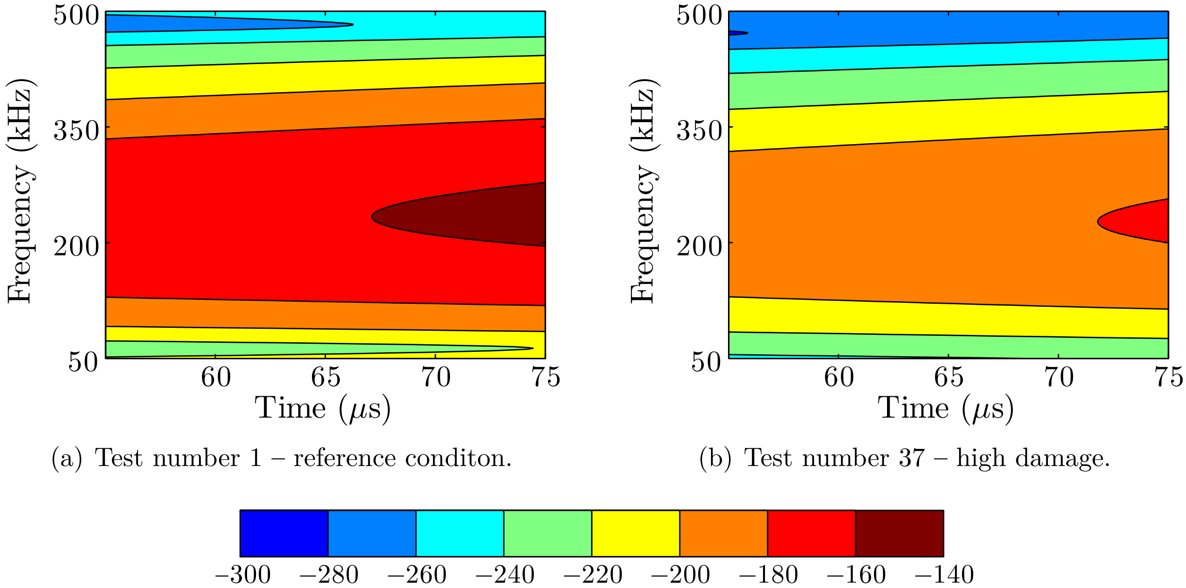

(a) Test number 1 – reference conditon.

(b) Test number 37 – high damage.

(c) PSD magnitude (dB – ref. 1 V×Hz^{-2}).

Source: Created by the author.

The result is an energy map matrix of each tested condition which is sensitive to structural changes. Singular value decomposition can be applied on the energy maps to generate matrix factorization:

$$E(l, f) = \mathbf{U}\mathbf{\Sigma}\mathbf{V}^T \tag{22}$$

where the superscript T refers to the transposed matrix, $\mathbf{U}$ and $\mathbf{V}$ are the left and right singular vectors of the STFT matrix and $\mathbf{\Sigma}$ contains the singular values in the diagonal form. The trace of matrix $\mathbf{\Sigma}$, which is the sum of its diagonal terms, carries information about the eigenvalues variation which is correlated to structural alteration (equation (4)). The normalized values of this damage index is presented in figure 7 confirming its sensitivity to the operational and structural scenarios tested.

APPENDIX D – Fuzzy Clustering Analysis

Cluster analysis is the process of grouping a set of objects using similar characteristics to evaluate the division. For the purpose of this work, a set of data is to be grouped into clusters taking into account the degree of similarity of its features. The method used in this work is the fuzzy c-means, which was first presented by Bezdek (1981):

$$\min_{f_{i,j},c_i} J = \sum_{j=1}^{N}\sum_{i=1}^{c} f_{i,j}^{p}\|x_j - C_i\|^2 \tag{23}$$

subjected to $0 <= f_{i,j} <= 1$,

$$\sum_{i=1}^{c} f_{i,j} = 1 \qquad \forall j \in \{1, 2, \cdots, N\}, \tag{24}$$

$$0 <= \sum_{j=1}^{N} f_{i,j} <= N \qquad \forall i \in \{1, 2, \cdots, c\}, \tag{25}$$

where f_{ij} is a function associated with the j^{th} object of the i^{th} cluster, C_i is the centroid of the i^{th} cluster, c is the number of clusters, and $p > 1$ is a constant that determines the relative positions of the clusters (normally set as 2), x_i is the feature index, N is the number of objects which depends on the number of datasets.

The distance norm can be written as:

$$\|x_j - C_i\|^2 = (x_j - C_i)^T \mathbf{A}(x_j - C_i) \tag{26}$$

where $\mathbf{A}$ is known as a norm-inducing matrix which usually is the identity matrix. Hence, one can only detect clusters with the same shape and orientation due to the same norm-inducing matrix for all clusters. The solution of the optimization problem described by equation (23) comes from the optimality equations via Lagrange multipliers. Details about this procedure can be found in (BEZDEK; PAL, 1992).